Abundance, distribution, and seasonality of cetaceans within the U.S. Exclusive Economic Zone around the Hawaiian Archipelago based on species distribution models

Elizabeth A. Becker, Karin A. Forney, Erin M. Oleson, Amanda L. Bradford, Ryan Hoopes, Jeff E. Moore, and Jay Barlow

U.S. DEPARTMENT OF COMMERCE
National Oceanic and Atmospheric Administration
National Marine Fisheries Service
Pacific Islands Fisheries Science Center

NOAA Technical Memorandum NMFS-PIFSC-131
https://doi.org/10.25923/9e50-d280

August 2022

Abundance, distribution, and seasonality of cetaceans within the U.S. Exclusive Economic Zone around the Hawaiian Archipelago based on species distribution models

Elizabeth A. Becker[1], Karin A. Forney[2], Erin M. Oleson[3], Amanda L. Bradford[3], Ryan Hoopes[1], Jeff E. Moore[4], and Jay Barlow[4]

[1] ManTech International Corporation, Inc.
Solana Beach, CA 92075

[2] Southwest Fisheries Science Center, National Marine Fisheries Service and Moss Landing Marine Laboratories, San Jose State University
7544 Sandholdt Rd. Moss Landing, CA 95039

[3] Pacific Islands Fisheries Science Center, National Marine Fisheries Service
1845 Wasp Boulevard Honolulu, HI 96818

[4] Southwest Fisheries Science Center, National Marine Fisheries Service
8901 La Jolla Shores Dr. La Jolla, CA 92037

NOAA Technical Memorandum NMFS-PIFSC-131

August 2022

U.S. Department of Commerce
Gina Raimondo, Secretary

National Oceanic and Atmospheric Administration
Richard W. Spinrad, Ph.D., NOAA Administrator

National Marine Fisheries Service
Janet Coit, Assistant Administrator for Fisheries

About this report

The Pacific Islands Fisheries Science Center of NOAA's National Marine Fisheries Service uses the NOAA Technical Memorandum NMFS-PIFSC series to disseminate scientific and technical information that has been scientifically reviewed and edited. Documents within this series reflect sound professional work and may be referenced in the formal scientific and technical literature.

Recommended citation

EA Becker, KA Forney, EM Oleson, AL Bradford, R Hoopes, JE Moore, J Barlow. 2022. Abundance, distribution, and seasonality of cetaceans within the U.S. Exclusive Economic Zone around the Hawaiian Archipelago based on species distribution models. U.S. Dept. of Commerce, NOAA Technical Memorandum NOAA-TM-NMFS-PIFSC-131, 45 p. doi:10.25923/9e50-d280

Copies of this report are available from

Pacific Islands Fisheries Science Center
National Marine Fisheries Service
National Oceanic and Atmospheric Administration
1845 Wasp Boulevard, Building #176
Honolulu, Hawai'i 96818

Or online at

https://repository.library.noaa.gov/

https://marinecadastre.gov/espis/#/

The content of this report, in part, fulfills the requirements of Interagency Agreements between the Bureau of Ocean Energy Management and the National Marine Fisheries Service (BOEM Agreement Number M17PG00024 and M17PG00025; NOAA Agreement Number NMFS-PIC-17-005), and the United States Navy and the National Marine Fisheries Service (Navy Agreement Number N0007017MP4C348; NOAA Agreement Number NMFS-PIC-17-006).

Table of Contents

List of Tables

List of Figures

Introduction

During the last two decades, there have been three systematic surveys of waters within the United States (U.S.) Exclusive Economic Zone (EEZ) around the Hawaiian Archipelago (henceforth "Hawaiian Islands EEZ" for brevity), all designed to provide information on the abundance of cetaceans within the entirety of this broad area. The first Hawaiian Islands Cetacean and Ecosystem Assessment Survey (HICEAS) was conducted from July to December 2002, and sighting data collected during this survey were used to derive the first quantitative abundance estimates for 19 cetacean species within the Hawaiian Islands EEZ (Barlow 2006). Two additional HICEAS surveys were conducted in the summer/fall of 2010 and 2017, and provided data used to update the original Hawaiian Islands EEZ design-based abundance estimates (Bradford et al. 2017; Bradford et al. 2021). In addition to the three HICEAS surveys, there have been smaller scale surveys within waters of the Hawaiian Islands EEZ focused on the Main Hawaiian Islands (MHI) and the Northwestern Hawaiian Islands, as well as survey effort from ships transiting through the area en route to other destinations, but the majority of these more localized efforts have also occurred during summer and fall.

Data from these surveys have been used to develop and update species distribution models (SDMs) for Hawaiian Islands EEZ cetaceans (Becker et al. 2012; Becker et al. 2021; Forney et al. 2015). SDMs have been recognized as valuable tools for estimating the density and distribution of cetaceans and assessing potential impacts from a wide range of anthropogenic activities (e.g., Gilles et al. 2011; Goetz et al. 2012; Hammond et al. 2013; Redfern et al. 2013). The most recent SDMs were developed using cetacean sighting data collected within waters of the Hawaiian Islands EEZ mainly during summer and fall from 2002–2017 (Becker et al. 2021). These models provide spatially-explicit density predictions at an approximate 9km x 9km grid resolution for the pantropical spotted dolphin (*Stenella attenuata*), striped dolphin (*S. coeruleoalba*), rough-toothed dolphin (*Steno bredanensis*), common bottlenose dolphin (*Tursiops truncatus*), Risso's dolphin (*Grampus griseus*), the pelagic stock of false killer whale (*Pseudorca crassidens*), short-finned pilot whale (*Globicephala macrorhynchus*), sperm whale (*Physeter macrocephalus*), and Bryde's whale (*Balaenoptera edeni*). Both pantropical spotted dolphins and common bottlenose dolphins are represented by several island-associated stocks within the Hawaiian Archipelago (see Carretta et al. 2020). To achieve sufficient sample sizes for modeling, the SDMs developed for these species were based on both pelagic and insular stock sightings, so the density patterns represented by the models likely represent a hybrid of the habitat characteristics of both insular and pelagic stocks (Becker et al. 2021). Abundance estimates from the current Hawaiian Islands EEZ spotted and bottlenose dolphin SDMs are thus not appropriate to use in the Stock Assessment Reports mandated by the U.S. Marine Mammal Protection Act.

High seasonal variability in cetacean abundance and distribution patterns have been observed and predicted from habitat models developed for waters in the California Current Ecosystem (Becker et al. 2014; Becker et al. 2017; Campbell et al. 2015; Forney and Barlow 1998), a region defined by high oceanic variability at multiple temporal and spatial scales (Hickey 1979). Dynamic oceanographic processes around the Hawaiian Islands occur on larger spatial and temporal scales than those of eastern boundary currents (Mann and Lazier 2006), but other than the migratory movements of mysticetes and sperms whales, little is known about the seasonal patterns of the non-migratory cetacean species. Seasonal distribution shifts have been described

for spinner dolphins, i.e., windward to leeward island shifts (Norris et al. 1994), but seasonal changes in abundance for this and other species have not been documented.

Until recently, systematic ship survey data in the winter months were limited to a single focused survey of the MHI from 6–24 February 2009 (Oleson 2009), and a few ship transits in proximity to the MHI. The MHI are a well-known migratory destination for North Pacific humpback whales (*Megaptera novaeangliae*) during winter and spring (Baker and Herman 1980; Craig and Herman 1997; Dawbin 1966), and their abundance has been estimated from mark-recapture methods based on the 3-year SPLASH project (Barlow et al. 2011; Calambokidis et al. 2008). For the majority of other cetaceans known to occur in waters of the Hawaiian Islands EEZ, not much is known about their abundance or distribution during winter.

To better understand the abundance and distribution of cetaceans in the winter months, a winter HICEAS survey was conducted within offshore waters around the MHI from 18 January to 12 March 2020 (Yano et al. 2018). The "Winter HICEAS" or WHICEAS 2020 survey was conducted as part of the Pacific Marine Assessment Program for Protected Species (PacMAPPS), a partnership between NOAA Fisheries, Bureau of Ocean Energy Management (BOEM), and the U.S. Navy. The primary objective of this line-transect survey was to collect cetacean sighting data to support the derivation of cetacean density estimates using both design- and model-based analyses and to investigate seasonal differences in abundance and distribution of cetaceans. A secondary objective of the survey was to derive stock-specific density estimates for insular stocks of various species within the main Hawaiian Islands. Given limitations in near-shore survey effort and small sample size, density estimates were explored only for pantropical spotted and common bottlenose dolphins. This report summarizes the results of the SDM effort. The design-based estimates are described separately in Bradford et al. (in press).

The SDM effort thus included three separate but related analyses:

1. Evaluate potential seasonal differences in species abundance;
2. Based on the results of the seasonal analysis, develop seasonally stratified habitat-based SDMs for species with seasonal differences and year-round density estimates for species without seasonal differences within waters of the Hawaiian Islands EEZ; and
3. If year-round sample sizes were sufficient, develop SDMs for the insular stocks of pantropical spotted and common bottlenose dolphins.

The resulting models provide spatially-explicit density predictions at ~9 km × 9 km resolution for the pelagic and insular stocks of pantropical spotted dolphins, the pelagic stock of common bottlenose dolphins, striped dolphins, rough-toothed dolphins, Risso's dolphins, short-finned pilot whales, and Bryde's whales, as well as monthly density predictions for humpback whales.

Methods

Survey data

Cetacean sighting data used to build the SDMs and investigate seasonal patterns of abundance were collected within waters of the Hawaiian Islands EEZ from 2000 to 2020 (Table 1) using line-transect methods (Buckland et al. 2001). Based on the survey periods and for the purposes of this analysis, "winter" was defined as January–March, and "non-winter" as April–December. Survey coverage in winter was limited to the offshore waters of the MHI, while in non-winter, effort from the combined surveys provided comprehensive coverage of waters within the Hawaiian Islands EEZ (Figure 1).

Table 1. Cetacean and ecosystem assessment surveys and effort conducted within the Hawaiian Islands EEZ during 2000–2020. "Winter" (January–March) surveys appear in bold.

Cruise number	Period in HI EEZ	Research vessel	Region
1616	Aug–Sept 2000	*McArthur*	Eastern Tropical Pacific[1]
1621	Jul–Dec 2002	*David Starr Jordan*	Hawaiian Archipelago
1622	Oct–Dec 2002	*McArthur*	Hawaiian Archipelago
1623	Aug–Sept 2003	*McArthur II*	Eastern Tropical Pacific[1]
1629	Aug–Nov 2005	*McArthur II*	Central Pacific Islands[1]
1631	Aug–Sept 2006	*McArthur II*	Eastern Tropical Pacific[1]
901	**Feb 2009**	***Oscar Elton Sette***	**Main Hawaiian Islands**
1001	**Jan 2010**	***Oscar Elton Sette***	**Mariana Islands[1]**
1004	May 2010	*Oscar Elton Sette*	Mariana Islands[1]
1641	Aug–Dec 2010	*McArthur II*	Hawaiian Archipelago
1642	Sep–Oct 2010	*Oscar Elton Sette*	Hawaiian Archipelago
1108	Oct 2011	*Oscar Elton Sette*	Palmyra Atoll[1]
1203	May 2012	*Oscar Elton Sette*	Palmyra Atoll[1]
1303	May–Jun 2013	*Oscar Elton Sette*	Northwestern Hawaiian Islands
1604	Jun–Jul 2016	*Oscar Elton Sette*	Main Hawaiian Islands
1705	Jul–Oct 2017	*Oscar Elton Sette*	Hawaiian Archipelago
1706	Aug–Dec 2017	*Reuben Lasker*	Hawaiian Archipelago
1901	April 2019	*Oscar Elton Sette*	Main Hawaiian Islands [2]
2001	**Jan–Mar 2020**	***Oscar Elton Sette***	**Main Hawaiian Islands**

[1] Transit portions located within the Hawaiian Islands EEZ were used.
[2] An equipment testing project.

The survey protocol was the same for all years (see Barlow 2006; Kinzey et al. 2000) with the exception of adjustments made to the collection of false killer whale data beginning in 2010 (Bradford et al. 2013; Bradford et al. 2017; Yano et al. 2018). Survey protocols are briefly summarized here. Each survey used a NOAA research vessel with a flying bridge and a team of six experienced visual observers who rotated through three positions. For each rotation, three observers stationed on the flying bridge of the ship visually searched for and recorded cetacean

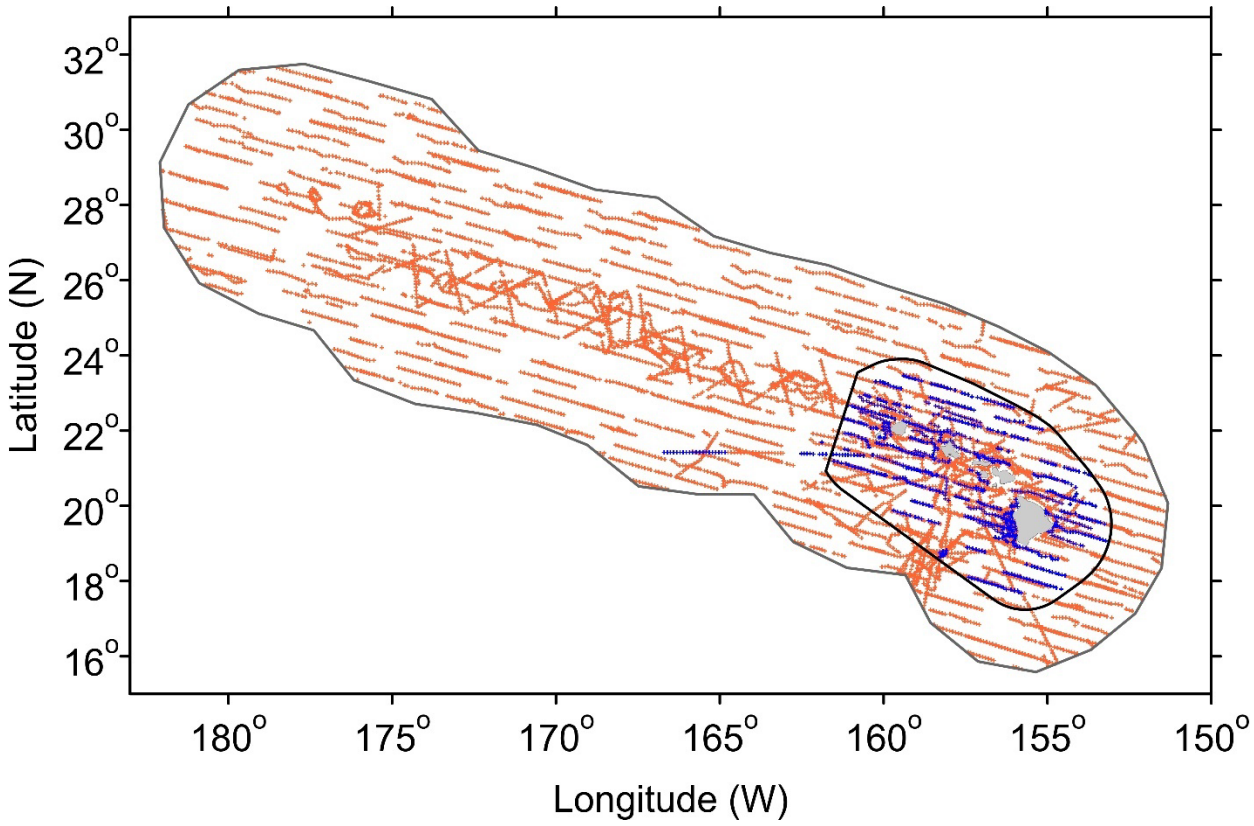

Figure 1. Effort segments from the 2000−2020 Southwest Fisheries Science Center and Pacific Islands Fisheries Science Center line-transect ship surveys used for modeling. The blue lines show on-effort modeling segments completed in Beaufort sea states of 0−6 in "winter" (January–March), and the orange lines in "non-winter" (April–December). The thin black line around the offshore waters of the main Hawaiian Islands depicts the boundary of the WHICEAS 2020 study area.

sightings between 0 and 90 degrees to port and starboard using standard line-transect protocols. Port and starboard observers searched with pedestal-mounted 25 × 150 binoculars and a center-stationed third observer searched by eye or with handheld 7 × 50 binoculars. When cetaceans were detected, the sighting was recorded along with the distance and direction of the sighting from the vessel, from which perpendicular sighting distance was calculated. When the sighting was within 3 nmi (5.6 km) of the trackline, the ship would typically divert from the transect line and go "off-effort" to approach the animals and enable more accurate estimation of group size and species identification. All observers independently provided best, high, and low group size estimates. Observers have a tendency to underestimate the size of cetacean groups (e.g., Gerrodette et al. 2018), so to account for this bias, correction factors were applied to the individual observer's "best" estimates. Correction factors for those observers who were calibrated during previous SWFSC surveys (Gerrodette and Forcada 2005) were applied directly, while an indirect regression-based calibration method was used to calibrate non-calibrated observers relative to the calibrated observers (Barlow 1995; Barlow and Forney 2007). To obtain a single group size estimate for each sighting, the weighted geometric mean of the calibrated

estimates of group size made by each observer (weighted by the inverse of the mean squared estimation error) was used.

Systematic survey effort was conducted along predetermined tracklines at an average survey speed of 18.5 km/hr. During transit between tracklines, transits to or from port, or deviations from pre-determined tracklines for other purposes, the visual observers generally maintained standard data collection protocols. Although such non-systematic effort is generally not used to derive encounter rates for design-based density estimates, it is incorporated into the SDM as the uneven distribution of effort can be accounted for within the statistical framework (Hedley and Buckland 2004).

Data preparation and predictor variables

To create samples for modeling, continuous portions of on-effort (systematic and non-systematic) survey tracklines were divided into approximate 10-km segments using methods described by Becker et al. (2010). The total number of species-specific sightings and associated calibrated group size estimates were assigned to each segment. Sighting data were truncated at 5.5 km perpendicular to the trackline to eliminate the most distant groups and to maintain consistency with the species-specific effective-strip-width (*ESW*) estimates derived by (Barlow et al. 2011) that were used in this study to estimate density.

Outputs from the Hybrid Coordinate Ocean Model (HYCOM; Chassignet et al. 2007) were used as dynamic predictor variables in the habitat models. HYCOM products include a global reanalysis that assimilates multiple sources of data in product development (including satellite and *in situ*), and outputs from HYCOM have been widely used and widely tested (https://www.hycom.org/). Daily averages for each variable served at the 0.08 degree (~ 9km) horizontal resolution of the HYCOM output were used in the models. The suite of potential dynamic predictors included sea surface temperature (SST) and its standard deviation, (sdSST), calculated for a 3 × 3-pixel box around the modeling segment midpoint), mixed-layer depth (MLD, defined by a 0.5˚C deviation from the SST), sea surface height (SSH), sd(SSH), salinity (SAL), and sd(SAL). Habitat covariates were derived based on the modeling segment's geographical midpoint. Water depth (m) was also included as a potential predictor, derived from the ETOPO1 1-arc-min global relief model (Amante and Eakins 2009) and obtained for the midpoint of each transect segment.

Explicit spatial terms (i.e., longitude and latitude) were not included in the suite of potential predictors offered to the models due to the seasonal heterogeneity of survey effort in the study area (Figure 1). SDMs that explicitly account for geographic effects have exhibited improved explanatory performance, but for most species they exhibit a decreased ability to predict abundance and distribution for novel conditions (Becker et al. 2018; Canadas and Hammond 2008; Forney et al. 2015; Hedley and Buckland 2004; Tynan et al. 2005; Williams et al. 2006).

For both the seasonal evaluation and subsequent development of the habitat-based SDMs, Generalized Additive Models (GAMs; Wood 2017) were developed in R (v. 3.4.1; R Core Team 2012) using the package "mgcv" (v. 1.8-31; Wood 2010).

A. Seasonal analysis within the WHICEAS study area

Given the seasonal effort bias (i.e., during the winter months effort was concentrated in offshore waters of the MHI; Figure 1), seasonal differences in species abundance were assessed by developing SDMs using only sighting data collected within the WHICEAS 2020 study area. For species with adequate sample sizes, two types of SDMs were developed to inform the seasonal evaluation as described below: (1) models were fit with a Julian date covariate to assess the potential for seasonal patterns of abundance, and (2) models were fit using the full suite of habitat covariates and then used to produce winter vs. non-winter abundance estimates for comparison.

1. Julian date model

The single-term GAMs were fit using the number of individuals in the group of the given species per transect segment (n_i, where i indexes the segments) as the response variable. The only predictor variable offered was the Julian day of each segment (x_i) included as a smooth function (f) fit with a cyclic cubic regression spline. The single term models were initially fit using both a Poisson and Tweedie distribution, but based on inspection of diagnostic plots of model residuals and quantiles, the Tweedie distribution was ultimately selected. The seasonal models therefore took the following form:

$$E(n_i) = \beta_0 + f(x_i) \text{ where } n_i \sim \text{Tweedie}(\phi, q). \quad (1)$$

Tweedie parameters ϕ (scale) and q (power) are estimated during model fitting and dictate the mean-variance relationship of the distribution such that $Var(X) = \phi E(X)^q$.

If the Julian date model identified a significant seasonal pattern in abundance (p-value < 0.05 and the functional plot was not flat within the 95% error bands), then seasonality was represented in the full Hawaiian Islands EEZ model using the Julian date covariate (Step B below).

2. Comparison of seasonal predictions from the habitat model

For species for which Julian date was not significant, a direct comparison of winter vs. non-winter densities predicted from a model developed using year-round survey data within the WHICEAS study area provided a secondary method of assessing potential seasonality. The habitat SDMs were fit using the number of individuals per transect segment as the response variable, which was assumed to follow a Tweedie distribution with a log link. Environmental covariates measured at each segment (x_{kj}, where k indexes the covariates) were included as smooth functions (f_k). Effort was accounted for by including an offset of the area covered (A_j; the product of the length of the segment, the truncation distance, and the number of sides surveyed, which generally = 2). Following the methods of Becker et al. (2016), the offset also included the probability of detection ($\hat{p}_j$; per segment derived from species-specific detection functions based on methods of Barlow et al. (2011)) and correction for detectability on the trackline ($\widehat{g(0)}_j$; using the method of Barlow (2015), which assumes that $\widehat{g(0)}_j = 1$ when average Beaufort sea state on the segment was 0, < 1% of the segments). These habitat-based models take the following form:

$$E(n_j) = A_j \hat{p}_j \widehat{g(0)}_j \, exp\left\{\beta_0 + \sum_{k=1}^{K} f_k(x_{kj})\right\} \text{ where } n_j \sim \text{Tweedie}(\phi, q). \quad (2)$$

Restricted maximum likelihood (REML) was used to optimize the parameter estimates (Wood 2010). The shrinkage approach of Marra and Wood (2011) was used to potentially remove terms from each model by modifying the smoothing penalty, allowing the smooth effect to be shrunk to zero (effectively performing model selection during fitting). To avoid overfitting, an iterative backwards selection process was used to remove variables that had p-values > 0.05 (Redfern et al. 2017; Roberts et al. 2016).

Spatially-explicit density values were derived from model predictions on the environmental conditions specific to the 2017–2020 winter and non-winter effort periods at 9-km^2 grid resolution within the WHICEAS study area. Density plots and abundance estimates generated from the predictions for the separate winter and non-winter periods were evaluated to see if seasonal differences were apparent. If the point estimates fell within the 95% confidence intervals, seasonal differences were not considered significant and new habitat-based SDMs for the Hawaiian Islands EEZ were developed in Step B using only the non-winter survey data. Winter survey data were excluded because the limited spatial sampling during those months could create a bias in models developed for the entire EEZ.

B. Habitat-based SDMs for the Hawaiian Islands EEZ

Similar to the seasonal GAMs, the habitat-based SDMs for the Hawaiian Islands EEZ followed Equation (2) above. Model performance was evaluated using established metrics, including the percentage of explained deviance, the area under the receiver operating characteristic curve (AUC; Fawcett 2005), the true skill statistic (TSS; Allouche et al. 2006), and visual inspection of predicted and observed distributions during the 2000–2020 cetacean surveys (Barlow et al. 2009; Becker et al. 2010; Becker et al. 2016; Forney et al. 2012). AUC discriminates between true-positive and false-positive rates, and values range from 0 to 1, where a score of > 0.5 indicates better than random discrimination. TSS accounts for both omission and commission errors and ranges from -1 to +1, where +1 indicates perfect agreement and values of zero or less indicate a performance no better than random. To calculate TSS, the sensitivity-specificity sum maximization approach (Liu et al. 2005) was used to obtain thresholds for species presence. In addition, the model-based abundance estimates for the Hawaiian Islands EEZ based on the sum of individual modeling segment predictions were compared to standard line-transect estimates derived from the same dataset used for modeling in order to assess potential bias in the habitat-based model predictions (Becker et al. 2018).

The final SDMs were used to predict spatially-explicit density values for the Hawaiian Islands EEZ study area, given the environmental conditions specific to the most recent four years of the study period (i.e., 2017–2020). Weekly model predictions were made based on the environmental conditions for every seventh day, thus taking into account the varying oceanographic conditions during 2017–2020. Daily predictions have been used for similar models developed for the California Current Ecosystem (Becker et al. 2018); however, given that the physical oceanographic properties of waters around the Hawaiian Archipelago are defined by larger-scale processes (Mann and Lazier 2006), a coarser temporal resolution was selected for this study area. The separate weekly predictions were then averaged across the 2017–2020 period

to produce spatial grids of average species density at 9-km^2 resolution within the study area. The final prediction grids thus provide a "multi-year average" of predicted weekly cetacean species densities. The weekly predictions were also used to create individual yearly abundance estimates for each of the four years. Density plots showing the most recent 2020 average predictions were developed for comparison to the multi-year average plots. The prediction grids were clipped to the boundaries of the 2,447,635-km^2 Hawaiian Islands EEZ study area.

The model-based abundance estimates were calculated as the sum of the individual grid cell abundance estimates, which were calculated by multiplying the cell area (in km^2) by the predicted grid-cell density, exclusive of any portions of the cells located outside the Hawaiian Islands EEZ or on land. Area calculations were completed using the R packages *geosphere* and *gpclib* in R (v2.15.0; R Core Team 2012).

Recently, Miller et al. (2022) developed techniques for deriving comprehensive measures of uncertainty in GAM predictions that account for the combined uncertainty from environmental variability, the GAM coefficients, *ESW,* and *g(0)*. These techniques include generating multiple daily density surfaces (for covariate rasters at each time slice) taking into account model parameter uncertainty (via posterior sampling from the model parameters) and providing a range of possible density estimates from which variance can be calculated. The Miller et al. (2022) methods were applied to estimate spatially-explicit measures of variance that accounted for uncertainty in environmental variability, the GAM parameters, and *ESW* for both the multi-year average and individual yearly abundance estimates. Uncertainty from *g(0)* was not incorporated into the pixel-specific estimates because the Miller et al. (2022) technique does not currently allow incorporation of *g(0*) variance when the method of Barlow (2015) that accounts for sea state is used, as in this study. Therefore, the pixel-based variance estimates are under-estimated to some degree, because they do not include sea-state specific *g(0)* variance estimates. However, our analysis includes the dominant sources of uncertainty to a greater extent than previous modeling studies (e.g., Becker et al. 2021).

Variance in *g(0)* and group size were subsequently incorporated into the variance of the study-area wide abundance estimates using the Delta method (Seber 1982). Variance in group size was estimated based on the variation in observed group sizes using standard statistical formulae. Uncertainty in *g(0)* was derived using the variance estimates for this parameter weighted by the proportion of survey effort conducted within each of the Beaufort sea state categories and estimated based on 10,000 bootstrap values (Becker et al. 2021). Variance for the multi-year and yearly study area abundance estimates thus included the combined uncertainty from environmental variability, the GAM parameters, *ESW, g(0)*, and group size.

For predictions averaged at a temporal resolution finer than yearly, the methods of Becker et al. (2021) were used to estimate uncertainty because the Miller et al. (2022) technique is currently not robust at small temporal scales. Variance in the monthly study area abundance and density estimates for humpback whale thus reflects the combined uncertainty from four sources: environmental variability, group size, *g(0)*, and *ESW*. Since GAM parameter uncertainty was not included in the combined uncertainty measures, the variance estimates for humpback whale are under-estimated to some degree, but the most important sources of uncertainty are accounted for.

C. Habitat-based SDMs for insular stocks

Habitat-based SDMs for the insular stocks of pantropical spotted and common bottlenose dolphins were developed following the methods described above for the Hawaiian Islands EEZ, but the study areas were limited to the combined range of the insular stocks around the MHIs for each species (Carretta et al. 2020).

Results

A. Seasonal analysis within the WHICEAS study area

Sighting data collected within the WHICEAS 2020 study area (Figure 1) and used to assess seasonal differences in abundance were limited for many of the species, particularly the pelagic stock of common bottlenose dolphin and the Bryde's whale, with too few sightings available to parameterize a GAM (Table 2). For the remaining species, when SDMs were fit with a single Julian date term to assess the potential for seasonal patterns of abundance, only the humpback whale model had a p-value < 0.05 and the functional plot was not flat within the 95% error bands (Figure 2). Deviance explained by the seasonal humpback whale GAM was 54.7%. For all the odontocetes, p-values for the seasonal SDMs exceeded 0.05 (range = 0.24–0.89) and the functional forms were flat within the 95% error bands.

Table 2. Number of sightings and average group size (Avg. GS) of cetacean species observed within the WHICEAS study area during the 2000–2020 shipboard surveys listed in Table 1 for which SDMs were developed to evaluate seasonal differences in abundance.

Common Name	Taxonomic Name	# Sightings	Avg. GS
Pantropical spotted dolphin (pelagic)	*Stenella attenuata*	32	60.24
Striped dolphin	*Stenella coeruleoalba*	31	44.34
Rough-toothed dolphin	*Steno bredanensis*	41	22.27
Common bottlenose dolphin (pelagic)	*Tursiops truncatus*	12	14.63
Risso's dolphin	*Grampus griseus*	23	22.03
Short-finned pilot whale	*Globicephala macrorhynchus*	62	26.62
Sperm whale	*Physeter macrocephalus*	30	8.68
Bryde's whale	*Balaenoptera edeni*	3	1.00
Humpback whale	*Megaptera novaeangliae*	84	5.40

When sighting data within the WHICEAS study area were then used to develop SDMs using the full suite of habitat covariates, depth was the only variable that entered the models for pantropical spotted dolphin, striped dolphin, and rough-toothed dolphin, making them ineffectual for evaluating seasonal differences in abundance or distribution. For the remaining species (the short-finned pilot whale, Risso's dolphin, and sperm whale), the best models included at least one dynamic variable (Table 3). Although winter sighting data available to parameterize the models were limited, the final models were used to make predictions on both the winter and non-winter periods of 2017–2020, in order to examine potential seasonal differences in distribution within the WHICEAS study area. Deviance explained by these models ranged from approximately 9% to 16% (Table 3). AUC values for all models were greater than 0.5, indicating that the models did better than random at discriminating between true-positive and false-positive results. The TSS values, which account for both omission and commission errors, ranged from 0.21 to 0.37.

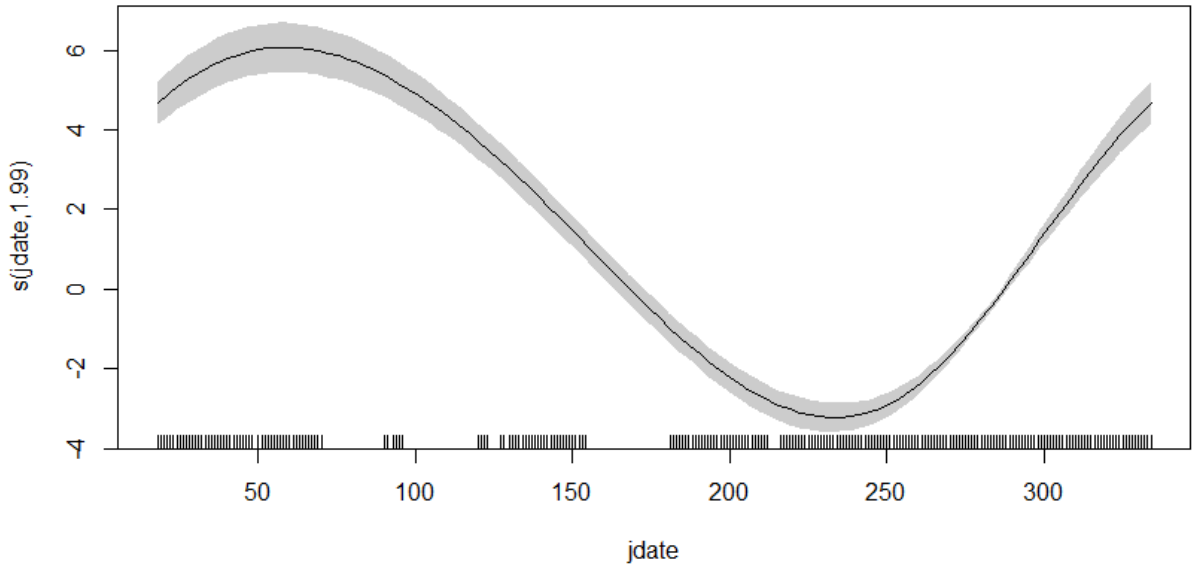

Figure 2. Functional plot for the humpback whale SDM built with Julian date (jdate) as the only predictor variable and number of whales as the response variable. The y-axis represents the term's spline function. The shading reflects 2× standard error bands (i.e., 95% confidence interval). The distribution of available Julian date values is shown on the rug plot of the x-axis.

Table 3. Summary of the three dynamic seasonal models built with the 2000–2020 survey data collected within the WHICEAS study area. The number of sightings available for model development are shown for the two seasonal periods. Variables are listed in the order of their significance and are as follows: MLD = mixed layer depth, SSH = sea surface height, and depth = bathymetric depth, All models were corrected for effort with an offset for the effective area searched (see text for details). Performance metrics included the percentage of explained deviance (Expl. Dev.), the area under the receiver operating characteristic curve (AUC), and the true skill statistic (TSS).

Species	# Winter	# Non-Winter	Predictor Variables	Expl. Dev.	AUC	TSS
Risso's dolphin	5	18	MLD	9.60	0.65	0.32
Short-finned pilot whale	14	48	depth + SSH + MLD	16.40	0.71	0.37
Sperm whale	11	19	MLD + depth	12.4	0.55	0.21

Density plots from the separate 2017–2020 winter and non-winter predictions show similar patterns of distribution for short-finned pilot whales and sperm whales, although regions of highest sperm whale density shift from the southeast to the northwest in the winter (Appendix A). The seasonal density plots for Risso's dolphin show more obvious differences, with an area of highest density in the northwest portion of the study area in winter that is not apparent in the other seasons (Fig 3a). The model-predicted WHICEAS study area abundance estimates for winter were very similar to point estimates derived from design-based methods (Bradford et al. in press), and the seasonal point estimates of abundance all fell within the 95% confidence intervals of the opposite season (Table 4). Although a significant seasonal difference was not

apparent from these results, the model-predicted winter abundance estimate for sperm whale was almost double that of non-winter (Table 4).

Table 4. Seasonal average (2017–2020) model-predicted estimates of abundance and density (animals per 100 km^2) and corresponding coefficient of variation (CV) within the WHICEAS study area. Seasonal estimates were predicted from the full model using the habitat characteristics for non-winter (April–December) and winter (January–March). Log-normal 95% confidence intervals (CIs) apply to abundance estimates only.

	Risso's Dolphin		Short-finned Pilot Whale		Sperm Whale	
	Non-Winter	Winter	Non-Winter	Winter	Non-Winter	Winter
Density	0.610	0.775	1.884	1.394	0.233	0.450
Abundance	2,464	3,130	7,609	5,630	944	1,817
CV	0.321	0.34	0.228	0.228	0.429	0.434
95% CI L	1,333	1,635	4,898	3,624	422	805
95% CI U	4,554	5,991	11,821	8,747	2,113	4,103

B. Habitat-based SDMs for the Hawaiian Islands EEZ

Given that a significant seasonal difference in abundance was evident for humpback whale, year-round survey data for the Hawaiian Islands EEZ were combined to develop a habitat-based SDM for this species that included the Julian date term. For all other species, only the non-winter survey data were used to develop habitat-based SDMs for the Hawaiian Islands EEZ. The number of sightings within the species-specific truncation distances and available for modeling ranged from 30 to 145 (Table 5).

Table 5. Number of sightings and average group size (Avg. GS) of cetacean species used to develop habitat-based density models for the Hawaiian Islands EEZ. Data were collected during the 2000–2020 shipboard surveys listed in Table 1. Winter survey data (i.e., January–March) were only included in the model for humpback whale. All sightings were made while on systematic and non-systematic effort in Beaufort Sea States ≤6 within the species-specific truncation distances (see text for details).

Common Name	Taxonomic Name	# Sightings	Avg. GS
Pantropical spotted dolphin (pelagic)	*Stenella attenuata*	50	70.96
Striped dolphin	*Stenella coeruleoalba*	61	42.93
Rough-toothed dolphin	*Steno bredanensis*	53	25.15
Common bottlenose dolphin (pelagic)	*Tursiops truncatus*	34	22.23
Risso's dolphin	*Grampus griseus*	30	21.71
Short-finned pilot whale	*Globicephala macrorhynchus*	83	28.19
Sperm whale	*Physeter macrocephalus*	92	9.46
Bryde's whale	*Balaenoptera edeni*	40	1.52
Humpback whale	*Megaptera novaeangliae*	145	2.98

The most commonly selected predictor variables in the Hawaiian Islands EEZ models were bathymetric depth and MLD (Table 6). The null model was selected for sperm whale, unlike previous modeling efforts for this study area (Becker et al. 2021). Since the null model does not provide spatially-explicit density predictions, further analyses from the sperm whale model were not made. Deviance explained by the models was variable, ranging from approximately 12% to 73% (Table 6). AUC values for all models were greater than 0.69, indicating that the models did a good job discriminating between true-positive and false-positive results. The TSS values, which account for both omission and commission errors, were more variable, ranging from 0.33 (striped and rough toothed dolphins) to 0.86 (humpback whale). The models for the pelagic stocks of pantropical spotted dolphin and bottlenose dolphin, Risso's dolphin, Bryde's whale, and humpback whale had observed:predicted density ratios close to 1, indicating that the sum of the segment-based density predictions was similar to standard line-transect estimates derived from the same segment observations used for modeling. The observed:predicted density ratios for the remaining species were within approximately 20% of the comparable design-based estimates.

Table 6. Summary of the final Hawaiian Islands EEZ models built with the 2000–2020 survey data. Variables are listed in the order of their significance and abbreviations are as follows: SST = sea surface temperature, SSTsd = standard deviation of SST, SAL = salinity, MLD = mixed layer depth, SSH = sea surface height, SSHsd = standard deviation of SSH, depth = bathymetric depth, J-date = Julian date. All models were corrected for effort with an offset for the effective area searched (see text for details). Performance metrics included the percentage of explained deviance (Expl. Dev.), the area under the receiver operating characteristic curve (AUC), the true skill statistic (TSS), and the ratio of observed to predicted density for the study area (Obs:Pred).

Species	Predictor Variables	Expl. Dev.	AUC	TSS	Obs:Pred
Pantropical spotted dolphin*	SSTsd + MLD + depth	14.8	0.69	0.39	0.95
Striped dolphin	MLD + depth	12.5	0.69	0.33	0.80
Rough-toothed dolphin	depth + SST	12.4	0.70	0.33	0.81
Bottlenose dolphin*	depth + SSTsd + SAL	40.8	0.89	0.69	0.95
Risso's dolphin	MLD + depth	18.4	0.76	0.45	0.99
Short-finned pilot whale	depth + SSH + SSHsd	19.7	0.77	0.48	0.83
Sperm whale	Null model	NA	NA	NA	NA
Bryde's whale	SST + MLD + SAL	14.0	0.77	0.47	0.99
Humpback whale	J-date + depth + SAL + SSH	73.2	0.97	0.86	0.98

*Pelagic stock

For those species for which seasonal differences in abundance were not evident (all but humpback whale), the multi-year average density surface maps generally captured observed distribution patterns as illustrated by actual sightings during the 2000–2020 surveys (Appendix B). Strong island associations were evident for pantropical spotted dolphin, rough-toothed dolphin, common bottlenose dolphin, and short-finned pilot whale (Figure B 1, Figure B 3, Figure B 4, Figure B 6), consistent with observations (Baird et al. 2008; Baird et al. 2009; Baird 2013) and predictions from prior density models (Becker et al. 2021; Forney et al. 2015). Unlike previous modeling efforts, the density outputs for pantropical spotted and common bottlenose dolphins are specific to the pelagic stocks of these species. Model-predicted distribution patterns

for 2020 were very similar to the multi-year average patterns (Appendix C). Differences in distribution patterns were most apparent for Bryde's whale, as in 2020 densities were generally higher throughout the study area and the regions with highest predicted density were concentrated in the northwest portion of the study area, different from the 2017–2020 multi-year average (Figs. B 7 and C 7).

Three sources of uncertainty (i.e., environmental variability, GAM parameters, and *ESW)* were combined to provide spatially-explicit measures of variance for the model-based density estimates (Appendices B and C). This represents a more comprehensive consideration of model uncertainty than that in previous modeling efforts that were based solely on uncertainty from environmental variability (Becker et al. 2021; Forney et al. 2015). Two additional sources of uncertainty were incorporated into the variance of the overall study area abundance estimates (i.e.,group size, and *g(0)*). Uncertainty estimates from the combination of environmental variability, GAM parameters, and ESW estimates ("CV_m (Model)" in Table 8) were variable, ranging from 0.099 (short-finned pilot whale) to 0.494 (Bryde's whale). Uncertainty due to the Beaufort-weighted g(0) values was quite high for both rough-toothed dolphin and the pelagic stock of common bottlenose dolphin. When combined, overall measures of CV for the study area abundance estimates were variable among the species, ranging from 0.215 (short-finned pilot whale) to 0.538 (Bryde's whale). Integration of uncertainty related to the GAM parameters and ESW into the modelling process has generally resulted in higher overall CVs for most modelled species.

The model-based 2017−2020 yearly abundance estimates showed some variation for all the species considered here, particularly for the pelagic stock of common bottlenose dolphin (Table 7). The abundance estimates were generally higher for most species than those estimated from previous modeling efforts (Becker et al. 2021), likely due in part to the use of calibrated group size estimates in the SDMs developed in this analysis.

Table 7. Multi-year (2017−2020) average and annual model-predicted estimates of abundance and density (100 km^{-2}), and corresponding coefficient of variation (CV) within the Hawaiian Islands EEZ for species exhibiting no seasonal difference. The yearly estimates were predicted from the full model using the habitat characteristics in that year. Log-normal 95% confidence intervals (CIs) apply to abundance estimates only.

Species	Period	Model Abundance	Model Density	CV	Low 95% CI	High 95% CI
Pantropical spotted dolphin (pelagic stock)	All years	71,433	2.920	0.358	36,136	141,209
	2017	73,667	3.010	0.283	42,769	126,886
	2018	69,116	2.824	0.272	40,939	116,688
	2019	75,806	3.097	0.279	44,329	129,634
	2020	67,313	2.750	0.269	40,096	113,005
Striped dolphin	All years	61,253	2.500	0.322	33,110	113,318
	2017	59,493	2.431	0.275	35,050	100,981

Species	Period	Model Abundance	Model Density	CV	Low 95% CI	High 95% CI
	2018	57,368	2.344	0.275	33,798	97,374
	2019	63,673	2.601	0.275	37,513	108,076
	2020	64,343	2.629	0.276	37,822	109,462
Rough-toothed dolphin	All years	82,071	3.350	0.501	32,476	207,406
	2017	86,068	3.516	0.487	34,857	212,519
	2018	82,481	3.370	0.496	32,882	206,893
	2019	76,126	3.110	0.487	30,830	187,970
	2020	83,915	3.428	0.486	34,025	206,958
Bottlenose dolphin (pelagic stock)	All years	25,598	1.050	0.447	11,083	59,124
	2017	25,857	1.056	0.556	9,356	71,464
	2018	31,576	1.290	0.637	10,064	99,075
	2019	20,309	0.830	0.546	7,457	55,311
	2020	24,669	1.008	0.566	8,774	69,361
Risso's dolphin	All years	7,007	0.290	0.349	3,607	13,614
	2017	7,437	0.304	0.321	4,027	13,736
	2018	6,738	0.275	0.323	3,633	12,497
	2019	6,907	0.282	0.346	3,570	13,362
	2020	6,979	0.285	0.340	3,649	13,348
Short-finned pilot whale	All years	19,029	0.780	0.215	12,549	28,855
	2017	17,237	0.704	0.232	11,009	26,989
	2018	19,854	0.811	0.232	12,680	31,087
	2019	19,644	0.803	0.257	11,957	32,272
	2020	19,242	0.786	0.232	12,289	30,129
Bryde's whale	All years	686	0.030	0.538	255	1,843
	2017	695	0.028	0.298	392	1,232
	2018	581	0.024	0.338	305	1,106
	2019	679	0.028	0.285	392	1,175
	2020	791	0.032	0.287	456	1,372

Table 8. Coefficient of variation (CV) for individual parameter estimates for the multi-year (2017−2020) average abundance estimates for the Hawaiian Islands EEZ. Sources of uncertainty incorporated into the total (tot) included environmental variability, effective strip width and GAM parameters ("Model"), g(0), and group size (gs).

Species	CV_m (Model)	CV_{g0}	CVgs	CVtot
Pantropical spotted dolphin	0.312	0.112	0.137	0.358
Striped dolphin	0.237	0.195	0.097	0.322
Rough-toothed dolphin	0.209	0.444	0.100	0.501
Common bottlenose dolphin	0.216	0.344	0.188	0.447
Risso's dolphin	0.278	0.173	0.120	0.349
Short-finned pilot whale	0.099	0.173	0.080	0.215
Bryde's whale	0.494	0.195	0.085	0.538

Since a significant seasonal difference in abundance was evident for humpback whale, the final SDM was used to derive spatially-explicit monthly density estimates based on the average of weekly predictions for oceanographic conditions spanning 2017–2020 (Appendix D). The average monthly density surface maps were generally consistent with documented humpback whale arrival and departure dates in the Hawaiian Islands EEZ, with peak abundance observed in late February through early April (e.g., Craig and Herman 1997; Johnston et al. 2007; Mobley et al. 2001). The model-based abundance estimates show peak numbers of humpback whales present in the Hawaiian Islands EEZ in March, with few whales present from June through October (Table 9).

Table 9. Monthly average (2017−2020) model-predicted estimates of humpback whale abundance and density (100 km^{-2}), and corresponding coefficient of variation (CV) within the Hawaiian Islands EEZ. Log-normal 95% confidence intervals (CIs) apply to abundance estimates only.

Month	Model Abundance	Model Density	CV	Low 95% CI	High 95% CI
January	1,918	0.0781	0.561	688	5,346
February	8,572	0.3488	0.560	3,077	23,877
March	9,250	0.3764	0.560	3,321	25,765
April	3,401	0.1384	0.561	1,221	9,476
May	404	0.0164	0.561	1,221	9,476
June-October	8*	0.0003	0.561	3	22
November	485	0.0197	0.561	174	1,352
December	4,465	0.1817	0.561	1,603	12,439

*Average for the 5 months.

Based on the functional plot for Julian date (Figure 2), peak numbers of humpback whales are expected to occur within the Hawaiian Islands EEZ from approximately February 19 through March 22, which is consistent with the peak timing documented in previous studies (Au et al. 2020). To obtain a single abundance estimate as needed for specific assessment and management

contexts, weekly predictions for this period were averaged to estimate the density and number of whales within the study area during 2020, the most recent year in the time series and the year of the WHICEAS effort (Appendix E). The resulting estimate of peak 2020 density was 0.461 whales/100 km^2 and abundance of 11,278 whales (CV=0.560, 95% CIs = 4,049−31,412). These estimates represent the peak abundance of humpback whales in the Hawaiian Islands EEZ during 2020, but may underrepresent the full abundance of whales that overwinter in the region because individual whales may not have very long residence times in Hawaii. Craig et al. (2001) found that for the majority of whales, 2 weeks or less elapsed between their first and last identification within the same field season, such that individual whales might use the area outside of the peak period. The total number of individuals in the Hawaii DPS might be more comprehensively estimated via mark-recapture analysis of photo-identification data.

C. Habitat-based SDMs for insular stocks

When data from all the 2000−2020 surveys were combined, there were still too few sightings available for developing SDMs for the insular stocks of common bottlenose dolphin (10 total sightings for all four insular stocks). The sample size for the insular stocks of pantropical spotted dolphin was small (34 total for all three insular stocks, with an average group size of 72.61), but allowed for the development of an SDM for the combined stock complex. Depth was the only predictor variable included in the final model, indicating that the greatest densities of dolphins occur in waters from approximately 1,500- to 3,500-m deep (Figure 3). Deviance explained by the GAM was 7.07%, with AUC and TSS values of 0.58 and 0.21, respectively, indicating better than random performance.

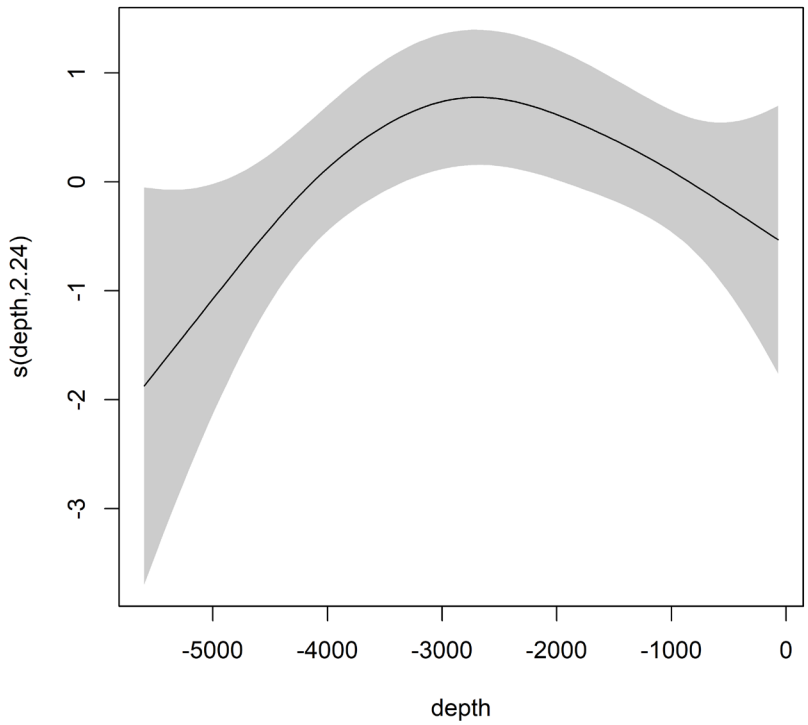

Figure 3. Functional plot for the SDM built for the three insular stocks of pantropical spotted dolphin. The y-axis represents the term's spline function. The shading reflects 2× standard error bands (i.e., 95% confidence interval).

Given that the SDM included only a static variable, model-based abundance estimates do not vary by year (Table 10), and it is not possible to predict changes in distribution using this model based on environmental variability. Density plots from the model predictions clearly show the influence of the single predictor variable, with highest predicted densities corresponding to depth contours around the islands (Appendix F).

Table 10. Average (2017−2020) model-predicted estimates of abundance and density (100 km^{-2}), and corresponding coefficient of variation (CV) for the three insular stocks of pantropical spotted dolphin. Log-normal 95% confidence intervals (CIs) apply to abundance estimates only.

Pantropical Spotted Dolphin Stock	Model Abundance	Model Density	CV	Low 95% CI	High 95% CI
Oahu	869	17.12	0.230	557	1,356
4-Islands	1,650	16.08	0.421	748	3,639
Hawaii Island	7,324	18.44	0.292	4,183	12,823

Discussion and Conclusions

The SDMs developed in this study are an improvement over prior modeling efforts for the Hawaiian Islands EEZ because they more accurately account for bias in group size estimates and they provide spatially-explicit variance estimates that incorporate additional sources of uncertainty not captured in previous estimates (i.e., GAM parameters and *ESW*). Unlike the previous models presented by Becker et al. (2021), the SDMs developed for both pantropical spotted and common bottlenose dolphins are stock specific, and thus more informative for management applications. The new humpback whale SDM provides the first fine-scale (9 × 9 km grid) monthly estimates of density and abundance for this species within waters of the Hawaiian Islands EEZ. Because explicit spatial terms (i.e., longitude and latitude) were not included in the suite of potential predictors offered to the models, they are better able to predict abundance and distribution under novel conditions (Becker et al. 2018). Becker et al. (2021) were able to develop SDMs for sperm whale and the pelagic stock of false killer whale; in the present analysis, the best sperm whale SDM was the null model, precluding evaluation of annual variability in stock abundance based on environmental variation and although there were four additional sightings of false killer whale on the 2020 WHICEAS survey, only two were identified to stock so the SDM for this species was not updated.

The multi-year distribution patterns predicted with these models were broadly similar to those predicted by Becker et al. (2021), particularly for striped dolphin, rough-toothed dolphin, Risso's dolphin, and short-finned pilot whale. The multi-year distribution patterns for Bryde's whale were the most dissimilar between the two studies, with areas of highest predicted density in different regions of the Hawaiian Islands EEZ. This result is not surprising given that great annual variability in distribution patterns has been documented for Bryde's whales in previous studies (Becker et al. 2021; Forney et al. 2015), likely reflecting a fluctuating distribution of the whales relative to habitat or prey distribution within the broader region.

For striped dolphin, rough-toothed dolphin, and short-finned pilot whale, the Hawaiian Island EEZ abundance estimates derived from the present models were greater than estimates from a recent modeling study (Becker et al. 2021), likely due in part to the use of calibrated group size estimates in the SDMs developed in this analysis. The previous model-based abundance estimates for pantropical and common bottlenose dolphins were based on both pelagic and insular stock sightings combined, and thus not directly comparable to the stock-specific estimates presented here. Abundance estimates for both Risso's dolphin and Bryde's whale were similar between the two modeling studies, particularly for 2017, the only predictive year of overlap between the two studies.

Dynamic oceanographic processes around the Hawaiian Islands occur on larger spatial and temporal scales than those of eastern boundary currents (Mann and Lazier 2006) so it is not surprising that a significant seasonal signal was not apparent for most of the species considered in this study. However, given data availability the seasonal analysis was limited to the WHICEAS study area; winter data collected throughout the Hawaiian Islands EEZ may be necessary to capture more subtle abundance and distribution shifts not apparent from the data available for this study. Although no significant seasonal difference was evident, predicted sperm whale abundance within the WHICEAS study area was substantially higher in winter than in summer (Table 4). Male sperm whales are known to migrate north in summer months and south

in winter in some regions (Whitehead 2003), which may partially account for the differences seen here.

The final SDM for humpback whale exhibited high explanatory power based on established metrics (Table 6). The model-predicted monthly density estimates are consistent with documented migration patterns in the Hawaiian Islands EEZ (Craig and Herman 1997; Johnston et al. 2007; Mobley et al. 2001) and thus provide a tool for assessing potential impacts to humpback whales on a finer temporal scale than previously available. Additional winter survey data collected throughout the Hawaiian Islands EEZ are required to cross validate and improve this SDM.

This study provides the first abundance estimates for the complex of MHI insular stocks of pantropical spotted dolphin. The functional plot for depth, the single predictor variable in the SDM, is consistent with sighting data collected from small boats that show peaks in depths from 1,500 to 3,500 m (Baird 2013). Given that predictions from this SDM produce density patterns that follow depth contours around the islands, it is not possible to assess potential differences in abundance between the leeward and windward sides of the islands. A previous habitat-based modeling effort using sightings collected from a variety of survey platforms suggested that spotted dolphins are less abundant on the windward sides of the islands (Pittman et al. 2016). However, this analysis did not produce stock-specific abundance estimates since the sighting data used to build the models were not specified by stock. Further, as noted by Pittman et al. (2016), the bias in survey effort (i.e., the majority of effort was concentrated on the leeward sides of the islands) may have biased the model predictions.

The design-based estimation of the WHICEAS 2020 survey data resulted in an estimate for the Hawaii Island stock (8,853, CV=0.72, 95% CI=2,487-31,508; Bradford et al. in press) that is similar in magnitude to the present model-based estimate (7,324, CV=0.29, 95% CI=4,183-12,823). Bradford et al. (in press) caution that their estimate (based on only two sightings) may be biased substantially upward if the density of spotted dolphins is higher on the leeward side of the island because the survey effort used in the estimation over represents the leeward side. The sample size of 34 sightings used in the present model-based estimation is also at the low end of what is considered a suitable sample size for SDMs (Becker et al. 2010; Forney et al. 2015; Wisz et al. 2008). Additional data are needed to resolve whether the windward sides of the islands are truly low-density regions, and if the model-based abundance estimates have an upwards bias. Given the limited range extent of the insular stocks, SDMs developed with finer scale sighting and oceanic data would help to improve our understanding of their distribution and abundance. Until then, these estimates represent a first attempt to assess insular spotted dolphin abundance, but the potential for bias may make them unsuitable for use in an assessment context.

Acknowledgements

We gratefully acknowledge the contributions of the survey coordinators, observers, acousticians, and the officers and crew aboard each of the PIFSC and SWFSC surveys that contributed data to these analyses. HICEAS 2002 was funded by SWFSC, and HICEAS 2010 was funded by SWFSC and PIFSC, with additional contributions by the Pacific Islands Regional Office and the NOAA Fisheries National Take-Reduction Program. HICEAS 2017 and WHICEAS 2020 were conducted as part of the Pacific Marine Assessment Program for Protected Species (PacMAPPS), a collaborative effort between NOAA Fisheries, the U.S. Navy, and the Bureau of Ocean Energy Management (BOEM) to collect data necessary to produce updated abundance estimates for all sighted cetaceans in Hawaiian waters. BOEM funding was provided via Interagency Agreement (IAA) M17PG00024, and Navy funding via IAAs with Chief of Naval Operations N45 (NEC-16-011-05) and Pacific Fleet Environmental Readiness Division (NMFS-PIC-07-006). Additional contributions were provided by the NMFS Office of Science and Technology, the National Take-Reduction Program, and the National Seabird Program. Survey of the Papahānaumokuākea Marine National Monument was conducted under research permits PMNM-2010-53 and PMNM-2017-17. Funding for the development of HYCOM has been provided by the National Ocean Partnership Program and the Office of Naval Research. Data assimilative products using HYCOM are funded by the U.S. Navy. Computer time was made available by the DoD High Performance Computing Modernization Program. The output is publicly available at https://hycom.org. This report was improved from reviews by Chip Johnson, Julie Rivers, and the Pacific Scientific Review Group.

Literature Cited

Allouche O, Tsoar A, Kadmon R. 2006. Assessing the accuracy of species distribution models: prevalence, kappa and the true skill statistic. Journal of Applied Ecology. 43:1223–1232.

Amante C, Eakins BW. 2009. ETOPO11 1 Arc-Minute Global Relief Model: Procedures, Data Sources And Analysis. Boulder, CO: National Oceanic And Atmospheric Administration, National Environmental Satellite, Data, and Information Service.

Au, W.W.L., Mobley, J., Burgess, W.C., Lammers, M.O. and Nachtigall, P.E. 2000. Seasonal and diurnal trends of chorusing humpback whales wintering in waters off western maui. Marine Mammal Science, 16: 530-544

Baird R. 2013. Odontocete Cetaceans Around the Main Hawaiian Islands: Habitat Use and Relative Abundance from Small-Boat Sighting Surveys. Aquatic Mammals. 39(3):253–269.

Baird RW, Webster DL, Mahaffy SD, McSweeney DJ, Schorr GS, Ligon AD. 2008. Site fidelity and association patterns in a deep-water dolphin: Rough-toothed dolphins (*Steno bredanensis*) in the Hawaiian Archipelago. Marine Mammal Science. 24(3):535–553.

Baird RW, Gorgone AM, McSweeney DJ, Ligon AD, Deakos MH, Webster DL, Schorr GS, Martien KK, Salden DR, Mahaffy SD. 2009. Population structure of island-associated dolphins: Evidence from photo-identification of common bottlenose dolphins (*Tursiops truncatus*) in the Main Hawaiian Islands. Marine Mammal Science. 25(2):251–274.

Baker CS, Herman LM. 1980. Migration and local movement of humpback whales (*Megaptera novaeangliae*) through Hawaiian waters. Honolulu, HI: Departments of Zoology and Psychology, University of Hawaii, Kewalo Basin Marine Mammal Laboratory.

Barlow J. 1995. The abundance of cetaceans in California waters. Part I: Ship surveys in summer and fall of 1991. Fishery Bulletin. 93:1–14.

Barlow J. 2006. Cetacean abundance in Hawaiian waters estimated from a Summer–Fall survey in 2002. Marine Mammal Science. 22(2):446–464.

Barlow J. 2015. Inferring trackline detection probabilities, g(0), for cetaceans from apparent densities in different survey conditions. Marine Mammal Science. 31(3):923–943.

Barlow J, Forney KA. 2007. Abundance and population density of cetaceans in the California Current ecosystem. Fishery Bulletin. 105:509–526.

Barlow J, Ferguson M, Becker E, Redfern J, Forney K, Vilchis I, Fiedler P, Gerrodette T, Ballance L. 2009. Predictive Modeling of Cetacean Densities in the Eastern Pacific Ocean. La Jolla, CA: National Oceanic and Atmospheric Administration, National Marine Fisheries Service, Southwest Fisheries Science Center.

Barlow J, Calambokidis J, Falcone EA, Baker CS, Burdin AM, Clapham PJ, Ford JKB, Gabriele CM, LeDuc R, Mattila DK et al. 2011. Humpback whale abundance in the North Pacific estimated by photographic capture-recapture with bias correction from simulation studies. Marine Mammal Science. 27(4):793–818.

Becker EA, Forney KA, Foley DG, Barlow J. 2012. Density and Spatial Distribution Patterns of Cetaceans in the Central North Pacific based on Habitat Models. La Jolla, CA: National Oceanic and Atmospheric Administration, National Marine Fisheries Service, Southwest Fisheries Science Center.

Becker EA, Forney KA, Foley DG, Smith RC, Moore TJ, Barlow J. 2014. Predicting seasonal density patterns of California cetaceans based on habitat models. Endangered Species Research. 23(1):1–22.

Becker EA, Forney KA, Oleson EM, Bradford AL, Moore JE, Barlow J. 2021. Habitat-based density estimates for cetaceans within the waters of the U.S. Exclusive Economic Zone around the Hawaiian Archipelago. Honolulu, HI: National Oceanic and Atmospheric Administration, National Marine Fisheries Service, Pacific Islands Fisheries Science Center.

Becker EA, Forney KA, Ferguson MC, Foley DG, Smith RC, Barlow J, Redfern JV. 2010. Comparing California Current cetacean–habitat models developed using in situ and remotely sensed sea surface temperature data. Marine Ecology Progress Series. 413:163–183.

Becker EA, Forney KA, Redfern JV, Barlow J, Jacox MG, Roberts JJ, Palacios DM. 2018. Predicting cetacean abundance and distribution in a changing climate. Diversity and Distributions. 2018:1–18.

Becker EA, Forney KA, Fiedler PC, Barlow J, Chivers SJ, Edwards CA, Moore AM, Redfern JV. 2016. Moving Towards Dynamic Ocean Management: How Well Do Modeled Ocean Products Predict Species Distributions? Remote Sensing. 8(2):149.

Becker EA, Forney KA, Thayre BJ, Debich AJ, Campbell GS, Whitaker K, Douglas AB, Gilles A, Hoopes R, Hildebrand JA. 2017. Habitat-Based Density Models for Three Cetacean Species off Southern California Illustrate Pronounced Seasonal Differences. Frontiers in Marine Science. 4(121):1–14.

Bradford AL, Yano KM, Oleson EM. In press.Why not? Estimating the Winter Abundance of Cetaceans around the Main Hawaiian Islands.

Bradford AL, Forney KA, Oleson EA, Barlow J. 2013. Line-transect abundance estimates of cetaceans in the Hawaiian EEZ. Honolulu, HI: National Oceanic and Atmospheric Administration, National Marine Fisheries Service, Pacific Islands Fisheries Science Center, Protected Species Division.

Bradford AL, Forney KA, Oleson EM, Barlow J. 2017. Abundance estimates of cetaceans from a line-transect survey within the U.S. Hawaiian Islands Exclusive Economic Zone. Fishery Bulletin. 115(2):129–142.

Bradford AL, Oleson EM, Forney KA, Moore JE, Barlow J. 2021. Line-transect Abundance Estimates of Cetaceans in U.S. Waters around the Hawaiian Islands in 2002, 2010, and 2017. Honolulu, HI: National Oceanic and Atmospheric Administration, National Marine Fisheries Service, Pacific Islands Fisheries Science Center.

Buckland ST, Anderson DR, Burnham KP, Laake JL, Borchers DL, Thomas L. 2001. Introduction to Distance Sampling: Estimating Abundance of Biological Populations. Oxford, United Kingdom: Oxford University Press.

Calambokidis J, Falcone EA, Quinn TJ, Burdin AM, Clapham PJ, Ford JKB, Gabriele CM, LeDuc R, Mattila D, Rojas-Bracho L et al. 2008. SPLASH: Structure of Populations, Levels of Abundance and Status of Humpback Whales in the North Pacific. Olympia, WA: Cascadia Research. Final report.

Campbell GS, Thomas L, Whitaker K, Douglas AB, Calambokidis J, Hildebrand JA. 2015. Inter-annual and seasonal trends in cetacean distribution, density and abundance off southern California. Deep Sea Research Part II: Topical Studies in Oceanography. 112:143–157.

Canadas A, Hammond PS. 2008. Abundance and habitat preferences of the short-beaked common dolphin *Delphinus delphis* in the southwestern Mediterranean: implications for conservation. Endangered Species Research. 4:309–331.

Carretta JV, Forney KA, Oleson EM, Weller DW, Lang AR, Baker J, Muto MM, Hanson B, Orr AJ, Huber H et al. 2020. U.S. Pacific Marine Mammal Stock Assessments: 2019. La Jolla, CA: National Oceanic and Atmospheric Administration, National Marine Fisheries Service, Southwest Fisheries Science Center.

Chassignet EP, Hurlburt HE, Smedstad OM, Halliwell GR, Hogan PJ, Wallcraft AJ, Baraille R, Bleck R. 2007. The HYCOM (HYbrid Coordinate Ocean Model) data assimilative system. Journal of Marine Systems. 65:60–83.

Craig AS, Herman LM. 1997. Sex differences in site fidelity and migration of humpback whales (*Megaptera novaeangliae*) to the Hawaiian Islands. Canadian Journal of Zoology.1923–1933.

Craig, A.S., Herman, L.M., and Pack, A.A. 2001. Estimating residence times of humpback whales in Hawai‘i. Report for the Hawaiian Islands Humpback Whale National Marine Sanctuary Office of National Marine Sanctuaries, NOAA, U.S. Dept of Commerce and the Department of Land and Natural Resources, State of Hawai‘i. June 2001.

Dawbin WH. 1966. The seasonal migratory cycle of humpback whales. In: Norris KS, editor. Whales, Dolphins and Porpoises. Berkeley, CA: University of California Press. p. 145–170.

Fawcett T. 2005. An introduction to ROC analysis. Pattern Recognition Letters. 27:861–874.

Forney KA, Barlow J. 1998. Seasonal patterns in the abundance and distribution of California cetaceans, 1991–1992. Marine Mammal Science. 14(3):460–489.

Forney KA, Becker EA, Foley DG, Barlow J, Oleson EM. 2015. Habitat-based models of cetacean density and distribution in the central North Pacific. Endangered Species Research. 27:1–20.

Forney KA, Ferguson MC, Becker EA, Fiedler PC, Redfern JV, Barlow J, Vilchis IL, Ballance LT. 2012. Habitat-based spatial models of cetacean density in the eastern Pacific Ocean. Endangered Species Research. 16(2):113–133.

Gerrodette T, Forcada J. 2005. Non-recovery of two spotted and spinner dolphin populations in the eastern tropical Pacific Ocean. Marine Ecology Progress Series. 291:1–21.

Gerrodette T, Perryman WL, Oedekoven CS. 2018. Accuracy and precision of dolphin group size estimates. Marine Mammal Science. 35(1):22–39.

Gilles A, Adler S, Kaschner K, Scheidat M, Siebert U. 2011. Modelling harbour porpoise seasonal density as a function of the German Bight environment: implications for management. Endangered Species Research. 14:157–169.

Goetz KT, Montgomery RA, Hoef JMV, Hobbs RC, Johnson DS. 2012. Identifying essential summer habitat of the endangered beluga whale *Delphinapterus leucas* in Cook Inlet, Alaska. Endangered Species Research. 16:135–147.

Hammond PS, Macleod K, Berggren P, Borchers DL, Burt L, Cañadas A, Desportes G, Donovan GP, Gilles A, Gillespie D et al. 2013. Cetacean abundance and distribution in European Atlantic shelf waters to inform conservation and management. Biological Conservation. 164:107–122.

Hedley SL, Buckland ST. 2004. Spatial Models for Line Transect Sampling. Journal of Agricultural Biological and Environmental Statistics. 9.

Hickey BM. 1979. The California Current System–hypotheses and facts. Progress in Oceanography. 8:191–279.

Johnston DW, Chapla ME, Williams LE, Matthila DK. 2007. Identification of humpback whale Megaptera novaeangliae wintering habitat in the Northwestern Hawaiian Islands using spatial habitat modeling. Endangered Species Research. 3:249–257.

Kinzey D, Olson P, Gerrodette T. 2000. Marine Mammal Data Collection Procedures on Research Ship Line-Transect Surveys by the Southwest Fisheries Science Center. La Jolla, CA: National Oceanic and Atmospheric Administration, National Marine Fisheries Service, Southwest Fisheries Science Center.

Liu C, Berry PM, Dawson TP, Pearson RG. 2005. Selecting thresholds of occurrence in the prediction of species distributions. Ecography. 28:385–393.

Mann KH, Lazier JRN. 2006. Dynamics of Marine Ecosystems: Biological-Physical Interactions in the Oceans. Malden, MA: Blackwell Publishing.

Miller DL, Becker EA, Forney KA, Roberts JR, Cañadas A, Schick RS. 2022. Characterising and estimating uncertainty in density surface models. PeerJ 10:e13950 https:// doi.org/10.7717/peerj.13950

Mobley JR, Spitz S, Grotefendt R. 2001. Abundance of Humpback Whales in Hawaiian Waters: Results of 1993–2000 Aerial Surveys. Honolulu, HI: Marine Mammal Research Commission.

Norris KS, Wursig B, Wells RS, Würsig M. 1994. The Hawaiian Spinner Dolphin. Berkeley, CA: University of California Press.

Oleson E. 2009. PIFSC Cruise Report CR-09-008, Oscar Elton Sette, Cruise 09-01 (SE-69), Issued 30 June 2009. Honolulu, HI: Pacific Islands Fisheries Science Center.

Pittman SJ, Winship AJ, Poti M, Kinlan BP, Leirness JB, Baird RW, Barlow J, Becker EA, Forney KA, Hill MC et al. 2016. Chapter 6: Marine Mammals. In: Costa BM, Kendall MS, editors. Marine Biogeographic Assessment of the Main Hawaiian Islands Bureau of Ocean Energy Management and National Oceanic and Atmospheric Administration OCS Study BOEM 2016-035 and NOAA Technical Memorandum NOS NCCOS 214. Silver Spring, MD: National Oceanic and Atmospheric Administration, Bureau of Ocean Energy Management. p. 227–265.

R Core Team. 2012. R: A language and environment for statistical computing. Vienna, Austria: R Foundation for Statistical Computing.

Redfern JV, McKenna MF, Moore TJ, Calambokidis J, Deangelis ML, Becker EA, Barlow J, Forney KA, Fiedler PC, Chivers SJ. 2013. Assessing the risk of ships striking large whales in marine spatial planning. Conservation Biology. 27(2):292–302.

Redfern JV, Hatch LT, Caldow C, DeAngelis ML, Gedamke J, Hastings S, Henderson L, McKenna MF, Moore TJ, Porter MB. 2017. Assessing the risk of chronic shipping noise to baleen whales off Southern California, USA. Endangered Species Research. 32:153–167.

Roberts JJ, Best BD, Mannocci L, Fujioka E, Halpin PN, Palka DL, Garrison LP, Mullin KD, Cole TVN, Khan CB et al. 2016. Habitat-based cetacean density models for the U.S. Atlantic and Gulf of Mexico. Scientific reports. 6:22615.

Seber GAF. 1982. The Estimate of Animal Abundance. London, United Kingdom: Charles Griffin & Company Limited.

Tynan CT, Ainley DG, Barth JA, Cowles TJ, Pierce SD, Spear LB. 2005. Cetacean distributions relative to ocean processes in the northern California Current System. Deep-Sea Research. 52:145–167.

Whitehead H. 2003. Sperm Whales Social Evolution in the Ocean. Chicago, IL: University of Chicago Press.

Williams R, Hedley SL, Hammond PS. 2006. Modeling Distribution and Abundance of Antarctic Baleen Whales Using Ships of Opportunity. Ecology and Society. 11(1).

Wisz MS, Hijmans RJ, Li J, Peterson AT, Graham CH, Guisan A. 2008. Effects of sample size on the performance of species distribution models. Diversity Distribution. 14:763–773.

Wood SN. 2010. Fast stable restricted maximum likelihood and marginal likelihood estimation of semiparametric generalized linear models. Journal of Royal Statistical Society. 73 (Part 1):3–36.

Wood SN. 2017. Generalized Additive Models: An Introduction with R. 2nd, editor. Boca Raton, FL: CRC Press Taylor a& Francis Group.

Yano KM, Oleson EM, Keating JL, Ballance LT, Hill MC, Bradford AL, Allen AN, Joyce TW, Moore JE, Henry A. 2018. Cetacean and Seabird Data Collected During the Hawaiian Islands Cetacean and Ecosystem Assessment Survey (HICEAS), July–December 2017. Honolulu, HI: National Oceanic and Atmospheric Administration, National Marine Fisheries Service, Pacific Islands Fisheries Science Center.

Appendix A: Seasonal species density maps for the WHICEAS study area

Maps depict predicted average winter (January–March) and non-winter (April–December) density (animals 100 km^{-2}) for the WHICEAS study area for models that included dynamic covariates: (a) Risso's dolphin, (b) short-finned pilot whale, and (c) sperm whale. Predictions were made from models developed using year-round survey data collected within the study area from 2000 to 2020, and then preditions made on the environmental conditions specific to the 2017–2020 seasonal periods (see text for more details). Density ranges are presented in quantiles specific to the seasonal period in order to assess potential differences in distribution. Abundance estimates are presented in Table 4, and no seasonal differences were identified.

(a) Risso's dolphin

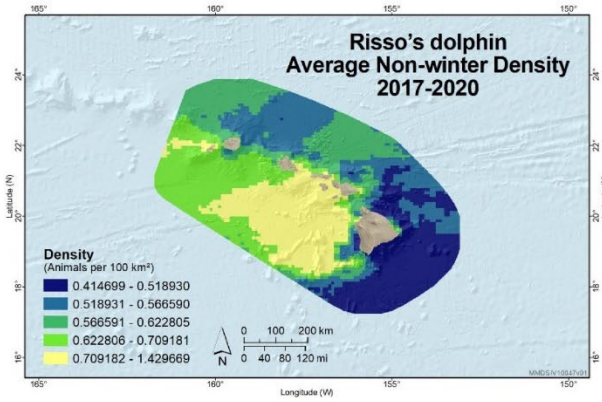

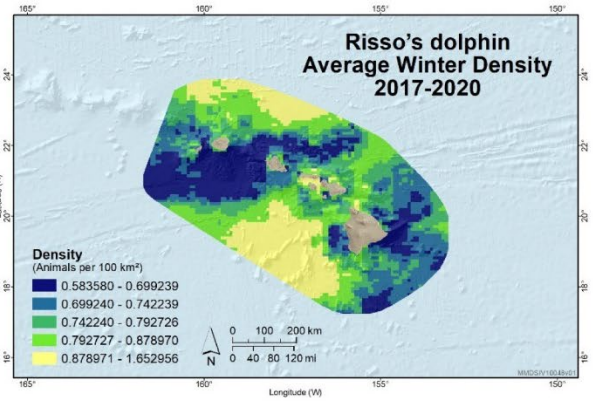

(b) Short-finned pilot whale

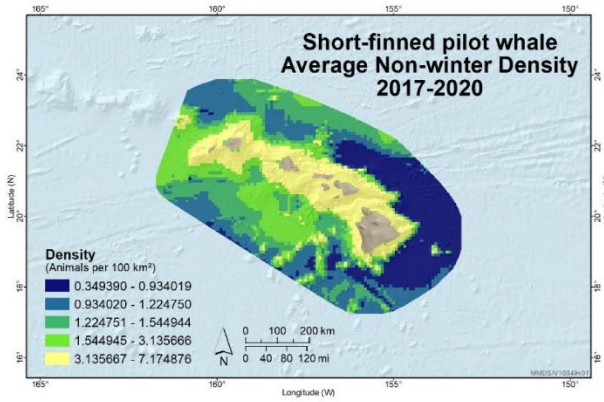

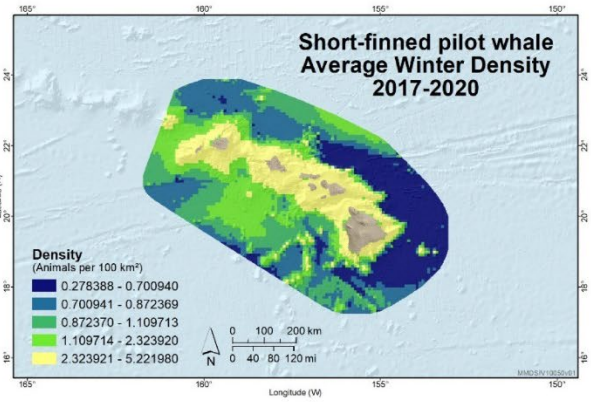

(c) Sperm whale

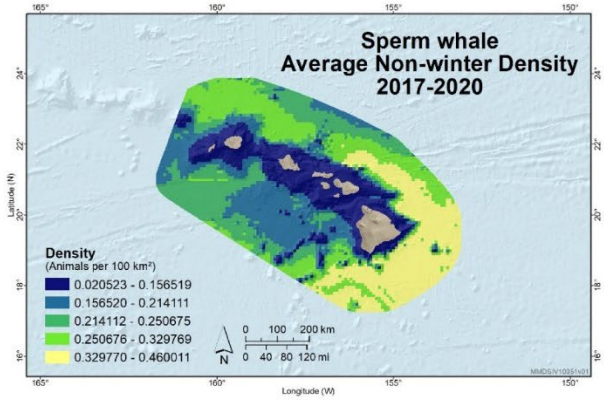

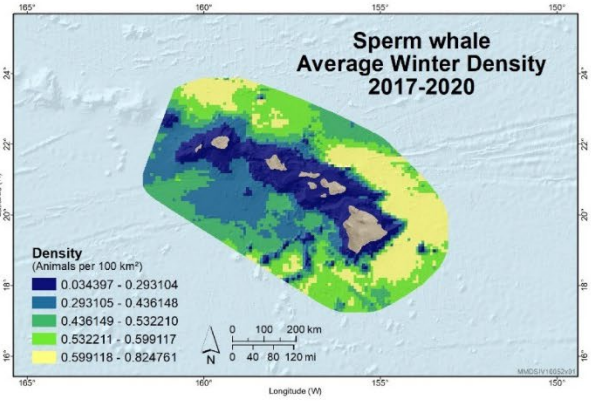

Appendix B: Species multi-year (2017–2020) average density maps

Maps depict predicted multi-year (2017–2020) average density (animals 100 km^{-2}) and spatially explicit estimates of the coefficient of variation (CV) in density for (1) the pelagic stock of pantropical spotted dolphin, (2) striped dolphin, (3) rough-toothed dolphin, (4) the pelagic stock of common bottlenose dolphin, (5) Risso's dolphin, (6) short-finned pilot whale, and (7) Bryde's whale. Predictions are shown for the Hawaiian Islands EEZ study area. Orange dots in the average plots show actual sighting locations from the 2000–2020 ship surveys.

(1) Pantropical spotted dolphin (pelagic stock)

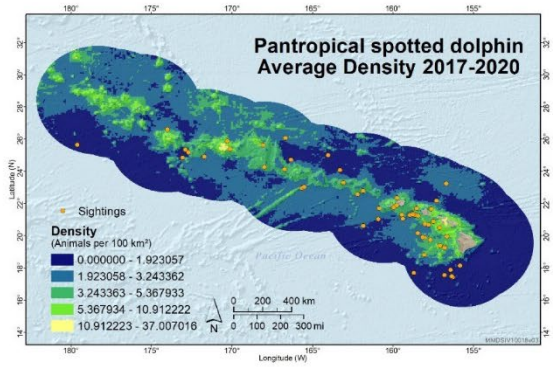

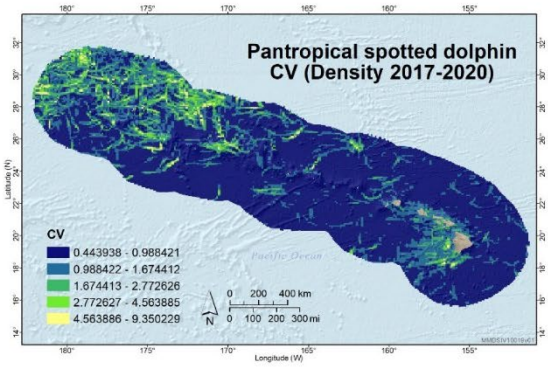

(2) Striped dolphin

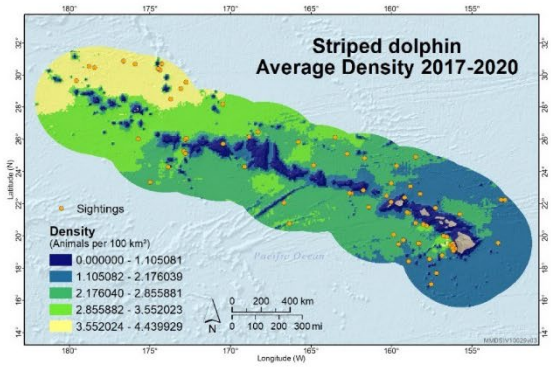

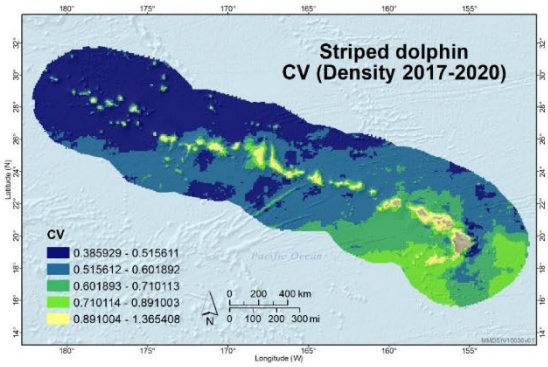

(3) Rough-toothed dolphin

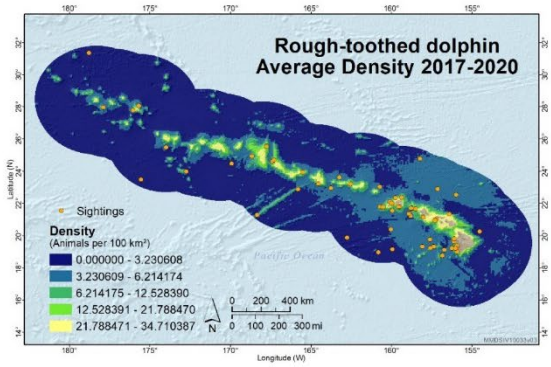

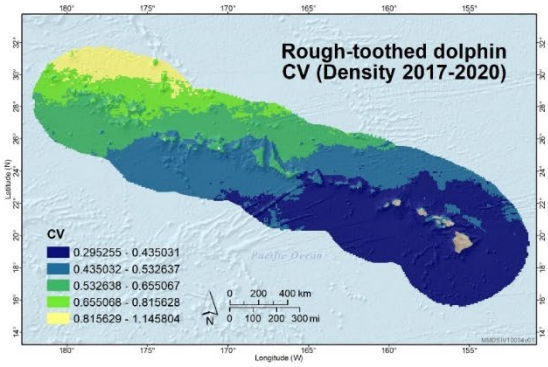

(4) Common bottlenose dolphin (pelagic stock)

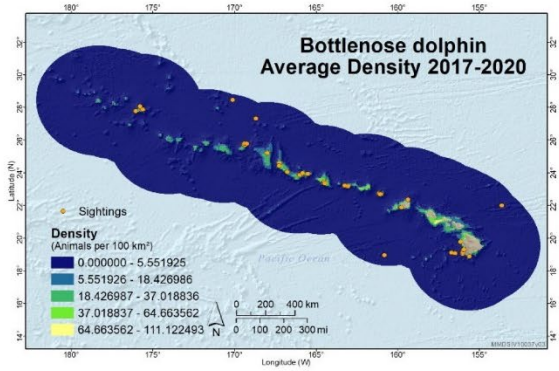

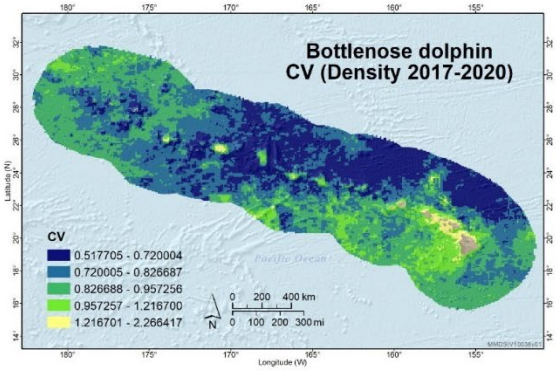

(5) Risso's dolphin

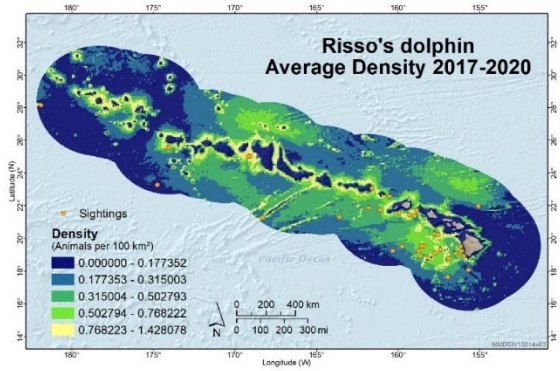

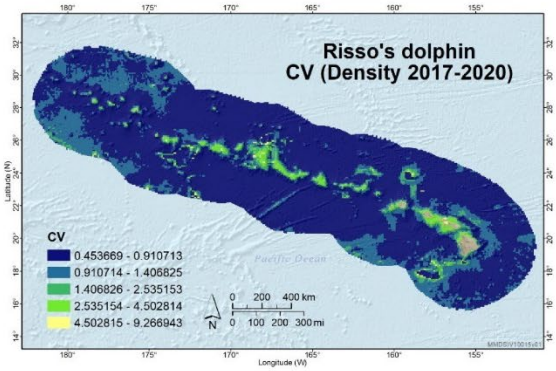

(6) Short-finned pilot whale

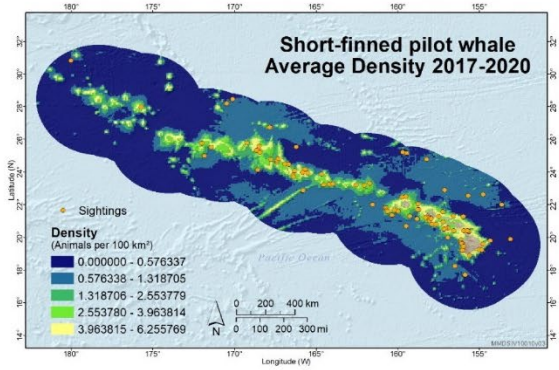

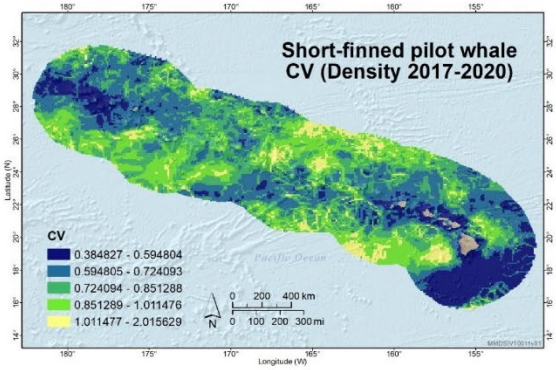

(7) Bryde’s whale

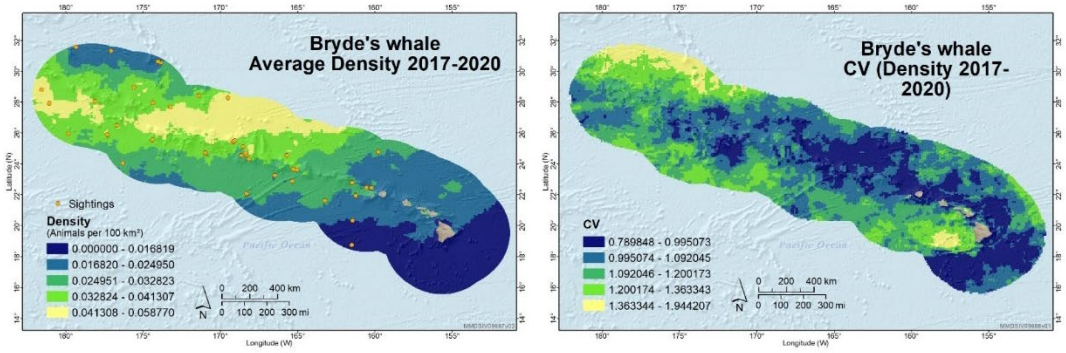

Appendix C: Species average 2020 density maps

Maps depict predicted 2020 average density (animals 100 km^{-2}) and the spatially explicit estimates of the coefficient of variation (CV) in density for (1) the pelagic stock of pantropical spotted dolphin, (2) striped dolphin, (3) rough-toothed dolphin, (4) the pelagic stock of common bottlenose dolphin, (5) Risso's dolphin, (6) short-finned pilot whale, and (7) Bryde's whale. Predictions are shown for the Hawaiian Islands EEZ study area.

(1) Pantropical spotted dolphin (pelagic stock)

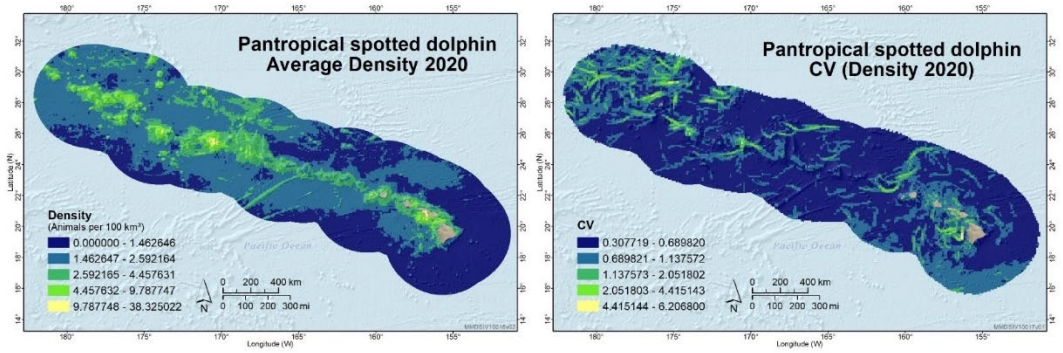

(2) Striped dolphin

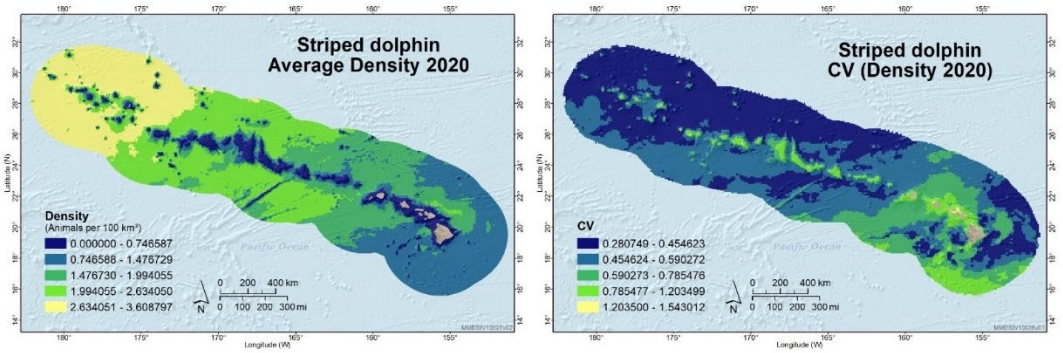

(3) Rough-toothed dolphin

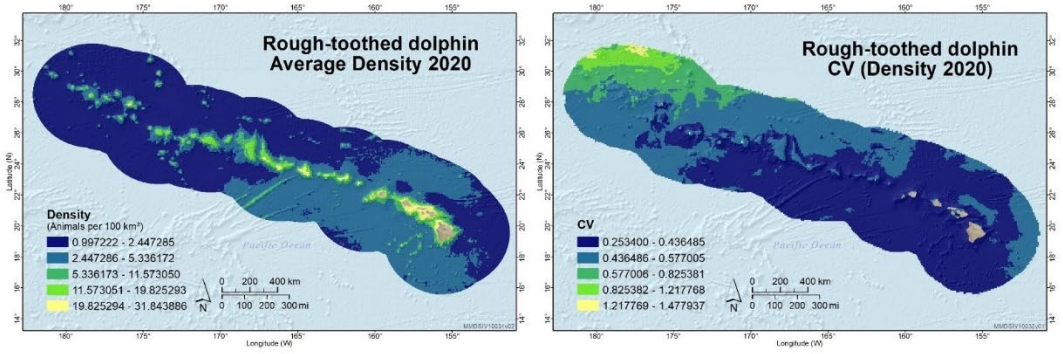

(4) Common bottlenose dolphin (pelagic stock)

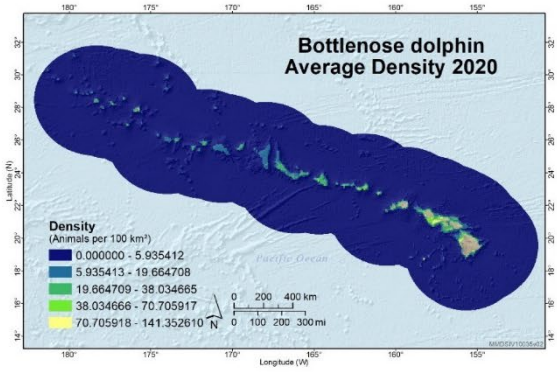

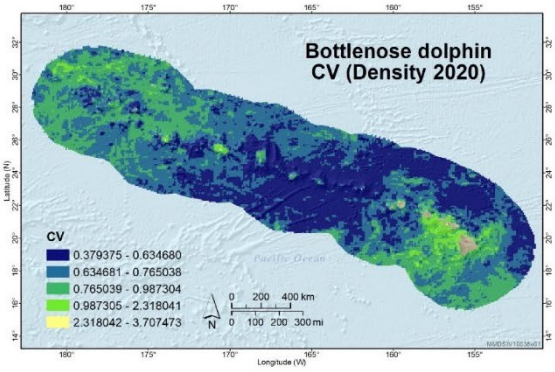

(5) Risso's dolphin

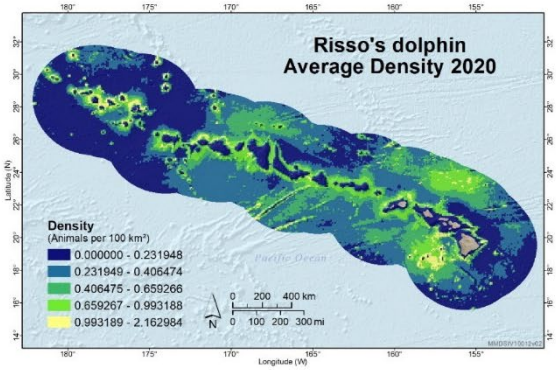

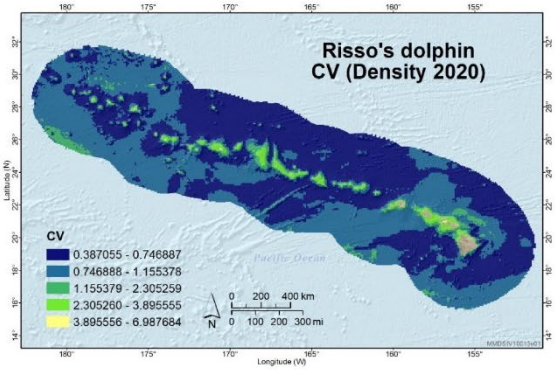

(6) Short-finned pilot whale

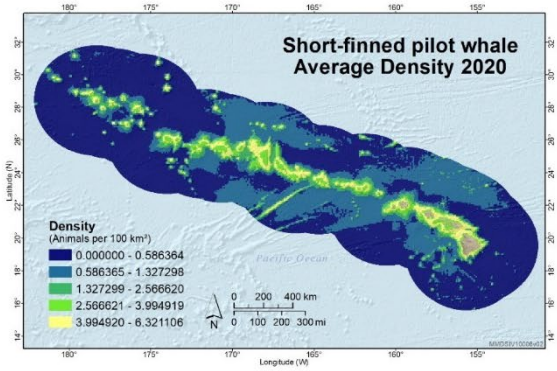

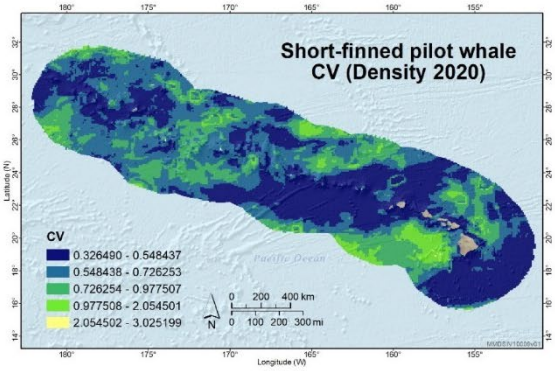

(7) Bryde’s whale

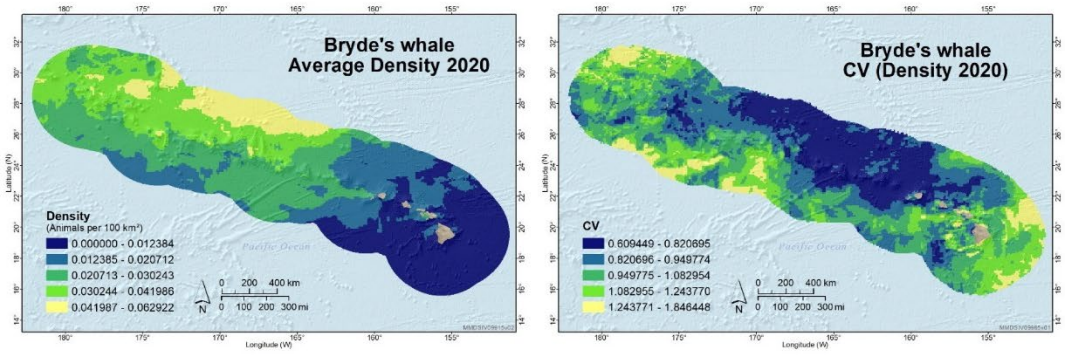

Appendix D: Humpback whale monthly average density maps

Maps depict predicted multi-year (2017–2020) average monthly density (animals 100 km^{-2}) and the coefficient of variation (CV) of density dervived from the habitat-based density model for humpback whale. The same density range is used for each month in order to assess differences in abundance. Predictions are shown for the Hawaiian Islands EEZ study area.

(1) January

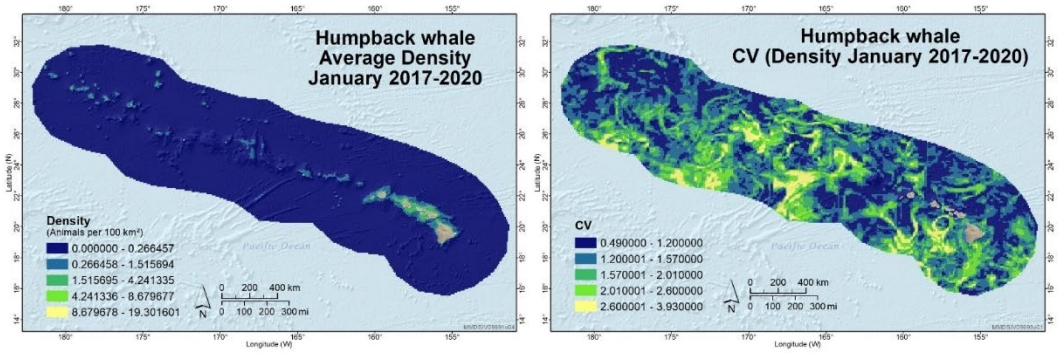

(2) February

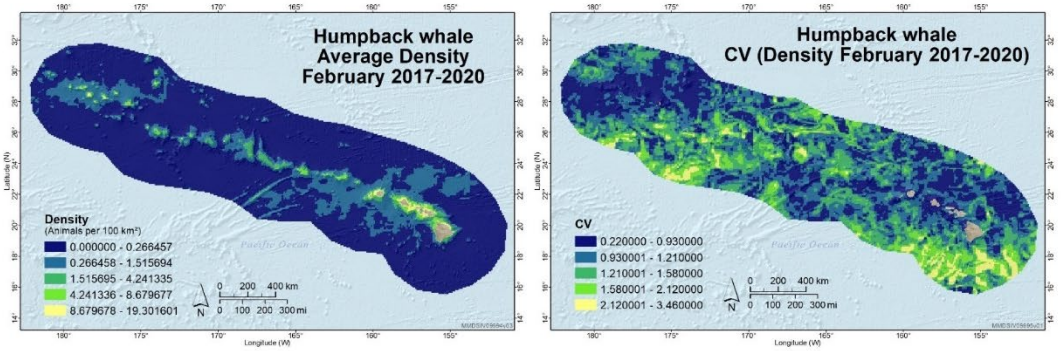

(3) March

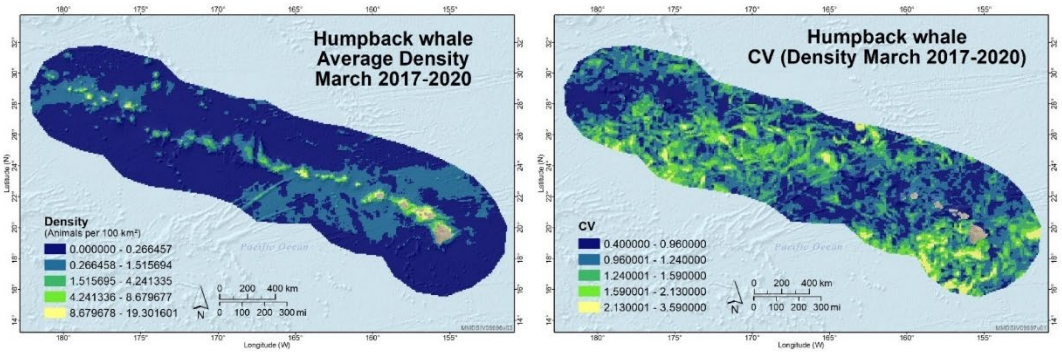

(4) April

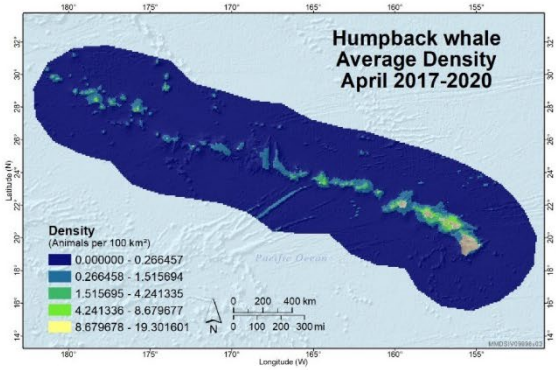

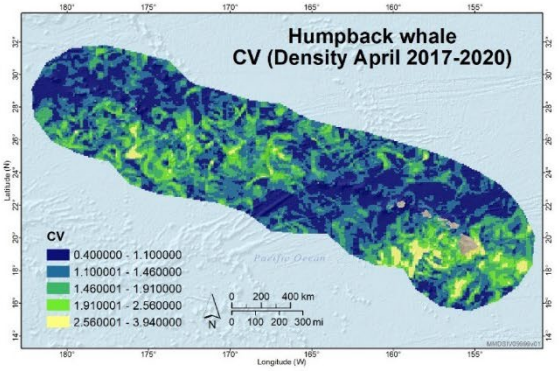

(5) May

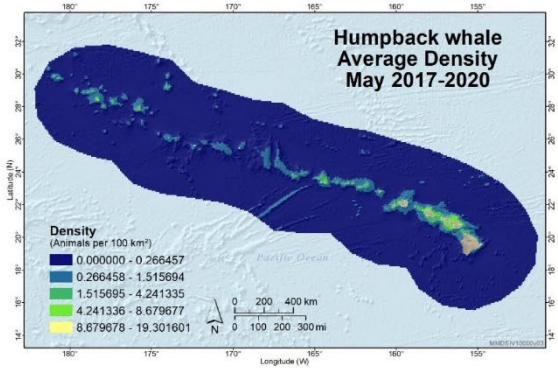

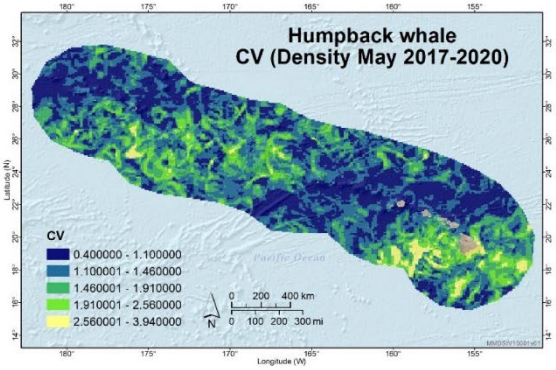

(6) June - October

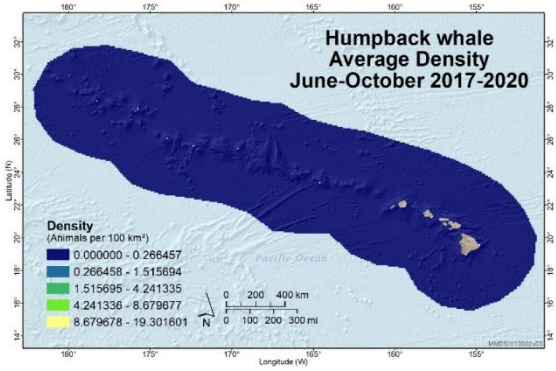

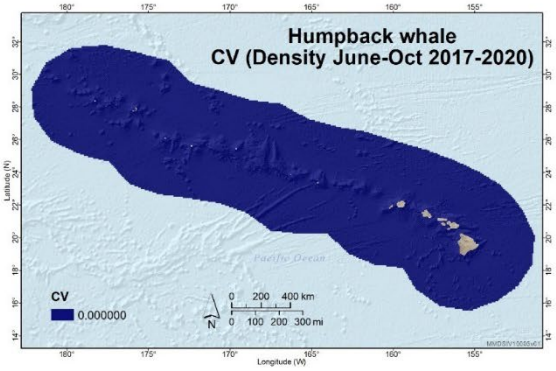

(7) November

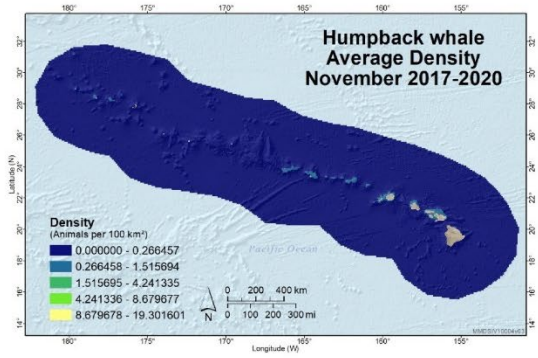

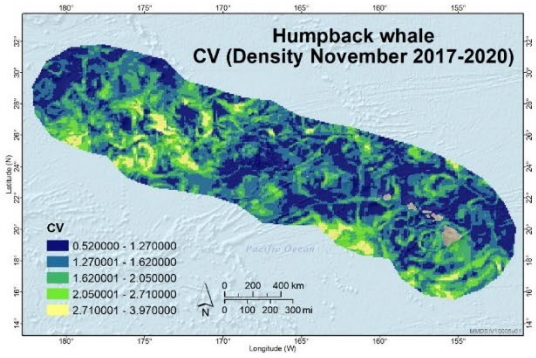

(8) December

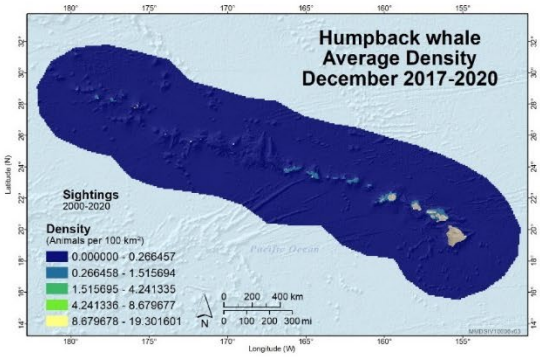

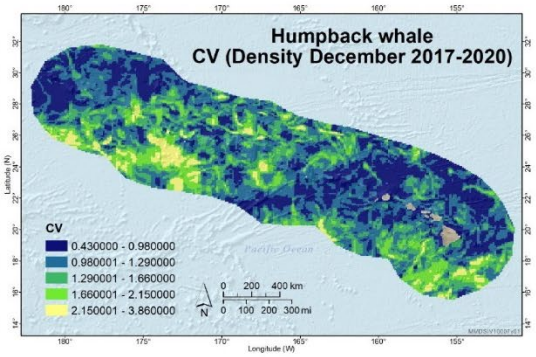

Appendix E: Humpback whale peak 2020 density maps

Maps depict predicted peak (February 19−March 22, 2020) density (animals 100 km^{-2}) and the coefficient of variation (CV) of density dervived from the habitat-based density model for humpback whale. Predictions are shown for the Hawaiian Islands EEZ study area.

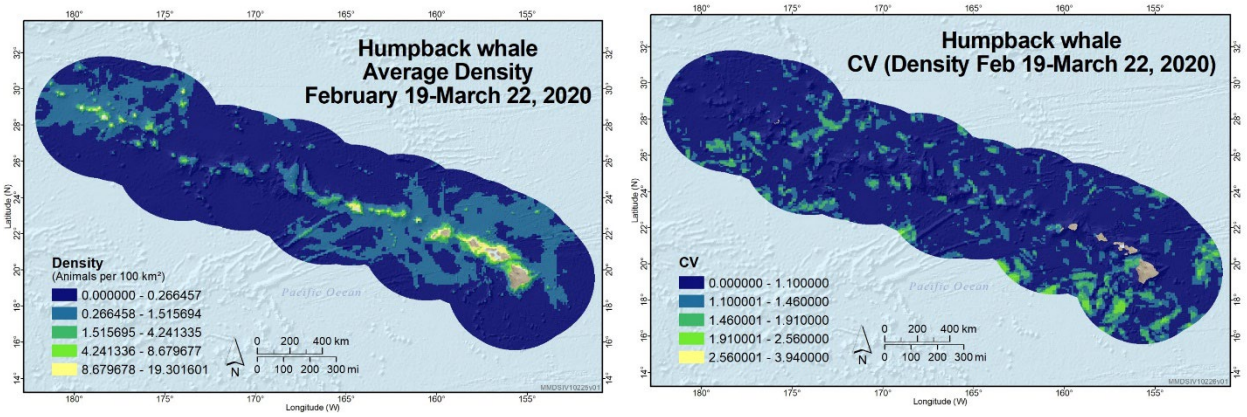

Appendix F: Density map for MHI insular pantropical spotted dolphin stock complex

Maps depict predicted multi-year (2017–2020) average density (animals 100 km^{-2}) and the coefficient of variation (CV) of density derived from the habitat-based density models for the combined insular stocks of pantropical spotted dolphin: Oahu stock, 4-Islands stock, and Hawaii Island stock. Predictions encompass the documented range of each stock (see Carretta et al. 2020). Orange dots in the average plot show actual sighting locations from the 2000–2020 ship surveys.